INTERFACE

royalsocietypublishing.org/journal/rsif

Research

Cite this article: Jiang J, Hastings A, Lai Y-C. 2019 Harnessing tipping points in complex ecological networks. *J. R. Soc. Interface* **16**: 20190345.
http://dx.doi.org/10.1098/rsif.2019.0345

Received: 17 May 2019
Accepted: 7 August 2019

Subject Category:
Life Sciences–Mathematics interface

Subject Areas:
evolution, biomathematics

Keywords:
tipping point, mutualistic networks, species recovery, ecosystem management, nonlinear dynamics, complex networks

Author for correspondence:
Ying-Cheng Lai
e-mail: ying-cheng.lai@asu.edu

Electronic supplementary material is available online at https://doi.org/10.6084/m9.figshare.c.4620539.

THE ROYAL SOCIETY PUBLISHING

Harnessing tipping points in complex ecological networks

Junjie Jiang[1], Alan Hastings[3,4] and Ying-Cheng Lai[1,2]

[1]School of Electrical, Computer, and Energy Engineering, and [2]Department of Physics, Arizona State University, Tempe, AZ 85287, USA
[3]Department of Environmental Science and Policy, University of California, One Shields Avenue, Davis, CA 95616, USA
[4]Santa Fe Institute, 1399 Hyde Park Road, Santa Fe, NM 87501, USA

JJ, 0000-0003-2930-7770; Y-CL, 0000-0003-0801-8830

Complex and nonlinear ecological networks can exhibit a tipping point at which a transition to a global extinction state occurs. Using real-world mutualistic networks of pollinators and plants as prototypical systems and taking into account biological constraints, we develop an ecologically feasible strategy to manage/control the tipping point by maintaining the abundance of a particular pollinator species at a constant level, which essentially removes the hysteresis associated with a tipping point. If conditions are changing so as to approach a tipping point, the management strategy we describe can prevent sudden drastic changes. Additionally, if the system has already moved past a tipping point, we show that a full recovery can occur for reasonable parameter changes only if there is active management of abundance, again due essentially to removal of the hysteresis. This recovery point in the aftermath of a tipping point can be predicted by a universal, two-dimensional reduced model.

1. Introduction

It has been increasingly recognized that complex networked systems can exhibit a tipping point at which an abrupt, irreversible and catastrophic transition from a normal state to an extinction state occurs when a system parameter passes through a critical point [1–18]. At the planetary scale, there is grave concern that the global ecosystem as a whole may be approaching a tipping point transition due to the human impact on the environment [12]. At the regional scale, the shutdown of the thermohaline circulation in the North Atlantic [2] is indication that the system has crossed a tipping point. At local scales, examples of tipping point transitions include global extinction of species in ecosystems [7,9,14,15] and the switch of shallow lakes from clear to turbid waters [3]. For complex ecological networks, to develop biologically viable management/control principles and strategies to remove the tipping point so as to delay the occurrence of global extinction is of broad interest. We note that, in the general field of controlling complex networks, in spite of a large body of literature on the linear controllability of complex networks [19–40], controlling *nonlinear* dynamical networks remains to be outstanding and is currently an active area of research [41–48].

A generic dynamical mechanism for the occurrence of a tipping point is saddle-node bifurcation. This produces a system which typically changes between one and multiple coexisting attractors as a parameter is varied. In low-dimensional systems, i.e. systems described by a few first-order nonlinear differential equations or maps, a previous work investigated how small perturbations can be used to drive the system to a desired attractor (tipping point control) [49]. Quite recently, it has been demonstrated for semiarid ecosystems that the phenomenon of an ecological 'ghost', a long transient phase during which the system maintains its stability, may be exploited to delay or prevent the occurrence of a tipping point [50]. Our problem is significantly more challenging as we seek to investigate how tipping points in real-world complex and nonlinear dynamical networks in ecology, which are typically high-dimensional with phase-space dimension of

the order of 100, can be managed or controlled. To be concrete, we focus on a large number of empirical pollinator–plant bipartite networks, whose dynamics are governed by mutualistic interactions [15,18,51–57]. To articulate a general management/control principle, we observe that a tipping point transition is the consequence of *gradual* changes in the system caused by a slow drift in the intrinsic parameter and/or external conditions. For example, human activities have been contributing to global warming, leading to a continuous deterioration of the environment. In an ecological network subject to harmful habitat changes, nodes and/or links in the network can gradually disappear, where the parameter of interest is the fraction of disappeared nodes. Another parameter is the species decay rate that can increase continuously. Environmental deterioration can also alter the pollination mutualism [58] and reduce the mutualistic interaction strength. For convenience, we call these parameters the 'environmental parameters'. When an environmental parameter drifts toward and through a critical point, species extinction at a global scale can occur. A realistic goal in managing a tipping point is then to alter the way that species extinction occurs: from massive extinction of all species (characteristic of a tipping point) to gradual extinction of individual species as the environmental parameter continues to increase, so that the occurrence of global extinction is substantially delayed. In this sense, we say that the tipping point has been removed through management or control.

While mathematical schemes can be conceived for tipping point control [49], in order to develop practical strategies that can actually be implemented in real ecological systems, one must take into account biological constraints. To appreciate this point, we consider two recent examples in harnessing ecosystems. The first is the controlled reversal of a cyanobacterial bloom in response to early warnings [59]. A sudden bloom of cyanobacteria in a lake or a reservoir can be devastating because it kills fish on a large scale and poses great toxicity risks for the environment. It is possible to predict regime shifts through resilience indicators, e.g. the statistical measures of some key ecosystem variables. The goal of control is to monitor the indicators to prevent the occurrence of any large scale bloom. Although, mathematically, control perturbations can be applied to any system parameters and/or variables, such strategies are often unrealistic due to the biological constraints. For the case of cyanobacteria, it was demonstrated experimentally that an intuitive but effective way to prevent a bloom is to stop or significantly reduce nutrient enrichment into the lake [59]. Another example is fisheries where drivers such as angling and shoreline development can lead to a regime shift [60]. The drivers can be externally manipulated through policy enforcement to prevent a large-scale extinction. Realistic management/control strategies include stipulating a rapid reduction in angling and/or introducing gradual restoration of the shoreline.

Guided by the biological constraint based principle, we seek practically realizable management strategies. For complex mutualistic networks, biological constraints mean that it is difficult to change many of the intrinsic parameters of the system. A viable strategy is to protect one particular pollinator species. We thus choose a 'targeted' species and maintain its abundance as the environmental parameter is increased. An equivalent strategy is to keep the decay rate of this species unchanged. We demonstrate that the abundance management can remove the tipping point and delay the occurrence of total extinction. The amount of delay depends on the particular species chosen as the target. The species can then be ranked in terms of management or control efficacy, and we find that the ranking is determined solely by the network structure, even though the intrinsic network dynamics are highly nonlinear. In the absence of abundance management, a hysteresis loop arises when attempting to restore the species population by improving the environment, i.e. by making the environmental parameter change in the direction opposite to that leading to an extinction. In particular, without abundance management, in order to revive the species abundances to the original level, the environmental parameter needs to be further away from the tipping point, i.e. the environment needs to be significantly more favourable than before the collapse. However, with abundance management the hysteresis loop disappears: species recovery begins at the point of global extinction. A striking role of abundance management is demonstrated when the environmental parameter is the mutualistic interaction strength, where species recovery is not possible without the abundance management, but a full recovery can be achieved with it.

In general, complex mutualistic networks are high-dimensional, nonlinear dynamical systems. There have been recent efforts to employ the mean-field approximation to reduce the system to a one-dimensional [61] or a two-dimensional [18] model for gaining understanding of the dynamics and for predicting the tipping point. We emphasize that our articulation of the management strategy is based on the full nonlinear dynamics of the original mutualistic network and realistic biological constraints, without using any mean-field type of reduced model. Nonetheless, we find that the species recovery point in the aftermath of a tipping point can be predicted reasonably well by a two-dimensional reduced model derived under the condition that abundance control/management is present.

2. Model

We study the approximately 60 real-world mutualistic pollinator–plant networks available from the Web of Life database (http://www.web-of-life.es), which were established based on empirical data collected from geographical regions across different continents and climatic zones. These networks differ greatly in their structure and in their numbers of pollinator and plant species. For those networks, a generic and ecologically realistic model describing the nonlinear dynamical evolution of the individual species abundances is available [15,18,54,55], which is based on the ubiquitous Holling type of dynamics in biology [62,63]. The model contains the following basic processes: intrinsic growth, intraspecific and interspecific competitions, and mutualistic interactions between the pollinators and plants. The abundances of the ith pollinator and the jth plant are denoted as A_i and P_j, respectively. The nonlinear differential equations governing the changes in A_i and P_j are

$$\frac{\mathrm{d}A_i}{\mathrm{d}t} = A_i\left(\alpha_i^{(A)} - \kappa_i - \sum_{j=1}^{S_A}\beta_{ij}^{(A)}A_j + \frac{\sum_{k=1}^{S_P}\gamma_{ik}P_k}{1+h\sum_{k=1}^{S_P}\gamma_{ik}P_k}\right) + \mu_A$$

$$\text{and}\quad \frac{\mathrm{d}P_i}{\mathrm{d}t} = P_i\left(\alpha_i^{(P)} - \sum_{j=1}^{S_P}\beta_{ij}^{(P)}P_j + \frac{\sum_{k=1}^{S_A}\gamma_{ik}A_k}{1+h\sum_{k=1}^{S_A}\gamma_{ik}A_k}\right) + \mu_P, \qquad (2.1)$$

where S_A and S_P are the numbers of pollinators and plants in the network and κ_i is the decay rate of the ith pollinator. The phase-space dimension of the whole networked system is $S_A + S_P$. In equation (2.1), γ_{ik} is the mutualistic interaction strength, which depends on the nodal degree K_i as $\gamma_{ik} = \varepsilon_{ik}\gamma_0/K_i^{\xi}$, where γ_0 is the average mutualistic strength, ε_{ik}'s are the elements of the network structural matrix: $\varepsilon_{ik} = 1$ if there is a mutualistic link between a pollinator and a plant species, $\varepsilon_{ik} = 0$ otherwise, and $0 \leq \xi \leq 1$ characterizes the trade-off between the interaction strength and the number of mutualistic links. For $\xi = 0$, the network topology will have no effect on the mutualistic interactions. Parameter α_i is the intrinsic growth rate in the absence of mutualistic interactions, whose value can vary slightly among the different species. For simplicity, we assume a common value of α for all pollinator species. The intraspecific and interspecific competitions are characterized by the parameters β_{ii} and β_{ij} $(i \neq j)$, respectively, where $\beta_{ii} \gg \beta_{ij}$. We assume $\beta_{ii} = 1$ and $\beta_{ij} = 0$. The parameter μ_A (μ_P) describes the immigration of pollinators (plants), which typically assumes a small value and has little effect on the network dynamics. When both mutualistic partners have a high abundance, the beneficial effect of the interactions on the population growth tends to saturate, which is characterized by the half saturation constant h.

Two remarks are in order.

First, mathematically, the parameters κ_i and α_i for pollinator species can be combined. However, the two parameters have different ecological meanings. In particular, α_i is the intrinsic growth rate or death rate of the species, and κ_i is the death rate caused by external factors such as excessive use of pesticides, climate warming or loss of habitat. To make the ecological meaning of these two parameters unambigious, it is useful to separate the two parameters.

The second remark concerns the choice of the parameter ξ. In the mathematical model, K_i is a divisor depending on the in-degree of the gain species in the network. Ecologically, the divisor characterizes the gain of a species from each connection. For a given species, a larger value of K_i indicates more connections, implying a weakened mutualistic effect associated with each individual connection. Note that we define γ_{ik} such that it depends on $1/K_i^{\xi}$. For $\xi = 0$, for any connection, we have $1/K_i^{\xi} = 1$, meaning that all the mutualistic connections are equally weighted. For $\xi = 1$, we have $1/K_i^{\xi} = 1/K_i$. In this case, the mutualistic interactions depend on the network topology. The two extreme cases are ecologically unrealistic. In our simulations, we set $\xi = 0.5$, a choice that was used in previous work [55,64].

3. Results

3.1. Management/control to delay collapse tipping point and enable species recovery

We present results with four representative networks: network A ($S_A = 61$ and $S_P = 17$ with the number of mutualistic links $L = 146$) from empirical data from Hicking, Norfolk, UK [65]; network B ($S_A = 42$, $S_P = 8$ and $L = 79$) from Hesteha-ven, Denmark [66]; network C ($S_A = 38$, $S_P = 11$ and $L = 106$) from Tenerife, Canary Islands [67]; and network D ($S_A = 44$, $S_P = 13$ and $L = 143$) from North Carolina, USA [68]. Figure 1*a*,*b* shows the structures of networks A and B, respectively. To demonstrate the beneficial role of abundance control/management, it is necessary to choose a bifurcation parameter. Our primary choice is γ_0, the nominal strength of the mutualistic edges, because deterioration of the environment (e.g. caused by global warming and climate change) can disrupt mutualism and, consequently, lead to population declines, reduced biodiversity and altered ecosystem functioning [64,69]. For an empirical mutualistic network, at the present data are not available to enable a quantitative assessment of the strength of each and every mutualistic interaction and the impact of environmental deterioration. As proof of principle, we vary the value of γ_0 systematically and study whether a reduction in γ_0 may lead to a tipping point and the role of abundance management in mitigating the tipping point.

As γ_0 is decreased from a relatively large value (e.g. $\gamma_0 = 3$) at which the system is fully functional, without abundance management, a tipping point occurs, at which the abundances of all species decrease to near zero, as shown by the brown curves in figure 1*c*,*d* for networks A and B, respectively.

In figure 1, we set the value of α to be negative so that, without mutualistic interactions, all species abundances will become zero. This is essential in making the mathematical model ecologically meaningful. Now apply the management strategy by which we protect a single pollinator species to maintain its abundance at a constant value (the light blue dashed horizontal lines in figure 1*c*,*d*). As a result, plants connected to the controlled pollinator experience a growth in their population, consequently elevating the equilibrium abundances, which in turn leads to a growth in the abundances of the pollinators connected to those plants, and so on. This generates a positive feedback loop in the system dynamics, which can delay the extinction of many species. Thus, while eventual global extinction still occurs, the process becomes gradual in the sense that the species disappear not at the same point, but they do so one after another, as indicated by the light blue dashed curves.

A striking phenomenon attesting to the benefits of control management arises when one attempts to restore the species by improving the environment so as to increase the value of γ_0 through the tipping point. Without the abundance management, species recovery from arbitrarily small abundance values (e.g. 10^{-4}) is impossible for any value of γ_0 in the range of interest, as indicated by the horizontal thick brown lines at $A \approx 0$ in figure 1*e*,*f* for networks A and B, respectively. However, abundance management enables a full recovery of all species abundances, as shown by the light blue dashed curves in figure 1*e*,*f*. While the controlled species is one that connects to the largest number of plants, we find that maintaining constant the abundance of a different species enables species recovery in a similar way.

To illustrate the generality of abundance management, we test different parameter settings from those in figure 1. Figure 2 shows the management results with increased values of the half saturation constant h and the intrinsic growth rates $\alpha_i^{(A)}$ and $\alpha_i^{(P)}$. We find that, in the absence of abundance management, the changes in the parameter values lead to a reduction in all species abundances. When abundance management is present, as the value of γ_0 is decreased from a relatively large value (e.g. $\gamma_0 = 3$), extinction of species becomes more gradual, as shown in figure 2*a*,*b*. When the direction of change in the value of γ_0 is reversed, species recovery begins to occur at the original extinction point, in sharp contrast to the case of absence of abundance management where species recovery is not

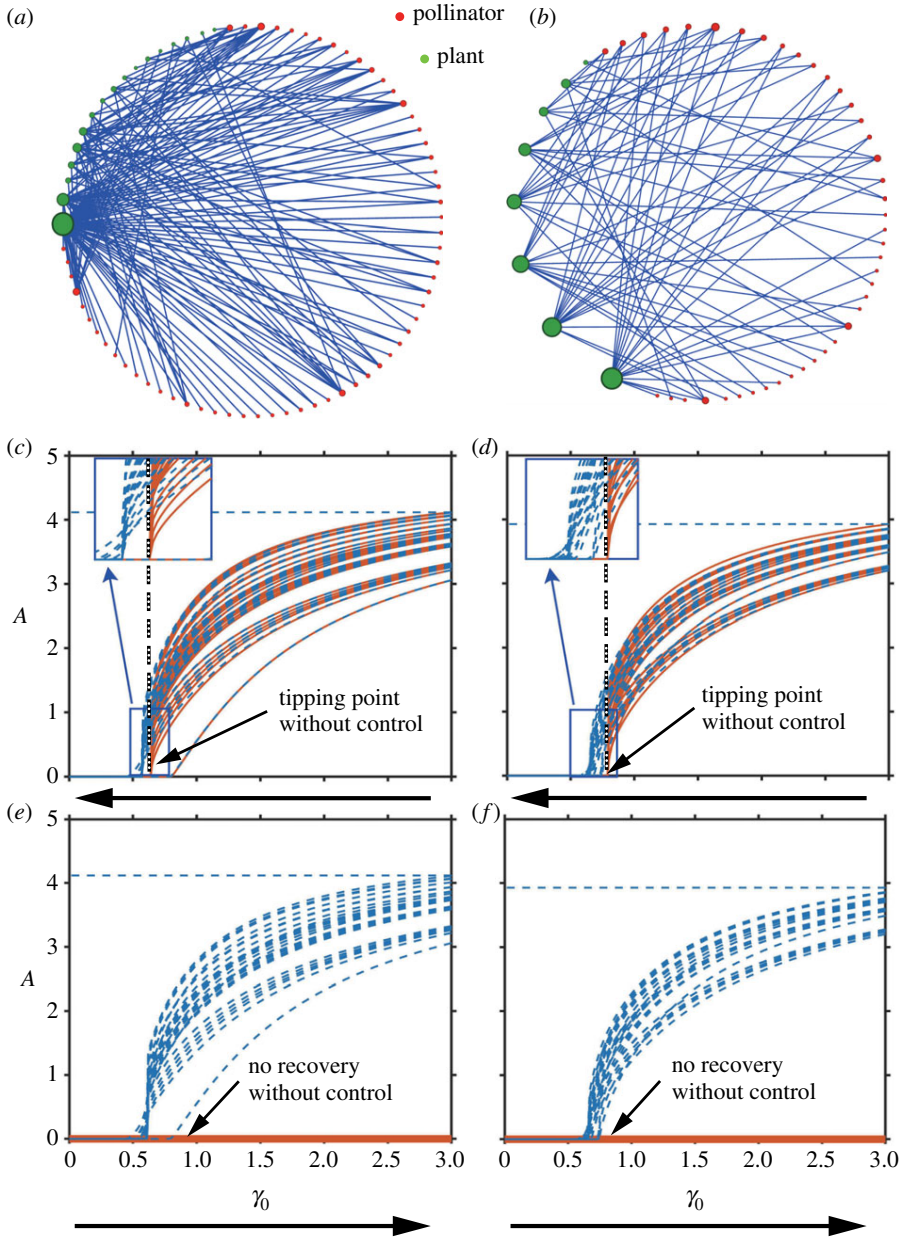

Figure 1. Tipping points in mutualistic networks and the role of abundance management. (*a*,*b*) The structures of two representative networks, where the red and green dots correspond to pollinator and plant species, respectively, and the size of a dot indicates the relative number of mutualistic links that this node has. The management strategy is to maintain the abundance of the pollinator species with the largest number of mutualistic connections at a constant level (the horizontal light blue dashed line). (*c*,*d*) In the absence of abundance management (brown curves), a tipping point occurs for networks *A* and *B*, respectively, as the bifurcation parameter γ_0 is decreased through a critical point. Regardless of whether abundance management is absent or present, global extinction is inevitable (light blue dashed curves). The difference is that the extinction event is abrupt and complete without abundance management, but it becomes gradual and benign with the management (insets). (*e*,*f*) When the direction of change in γ_0 is reversed as one attempts to recover the species by improving the environment, species recovery is not possible without abundance management (the thick brown lines at $A \approx 0$). Management enables a full recovery of all species once the value of γ_0 becomes larger than that associated with global extinction. The parameter values used in the computations are $h = 0.2$, $t = 0.5$, $\beta_{ii}^{(A)} = \beta_{ii}^{(P)} = 1$, $\beta_{ij}^{(A)} = \beta_{ij}^{(P)} = 0$, $\alpha_i^{(A)} = \alpha_i^{(P)} = -0.3$, $\kappa_i = 0$ and $\mu_A = \mu_P = 0.0001$. (Online version in colour.)

possible. Through extensive computations, we find that the phenomenon of control enabled species recovery occurs in wide parameter regions.

3.2. Management/control to delay collapse tipping and remove hysteresis loop

We study the system dynamics when the bifurcation parameter is the decay rate. For simplicity, we assume that the decay parameters for all the pollinators have an identical value: $\kappa_i \equiv \kappa$. We set $\gamma_0 = 1$. Generally, we assume there is a qualitative correspondence between κ and the state of the environment, in the sense that a deteriorating environment for species corresponds to an increased value of κ, and vice versa. As the value of κ is increased, species extinction can occur. A tipping point of the system is defined as the critical value of κ at which all species become extinct abruptly. In the following, we present results with two management strategies: maintaining the abundance of a particular pollinator (abundance management) or keeping its decay rate constant (decay rate management), and demonstrate that management can effectively remove the tipping point.

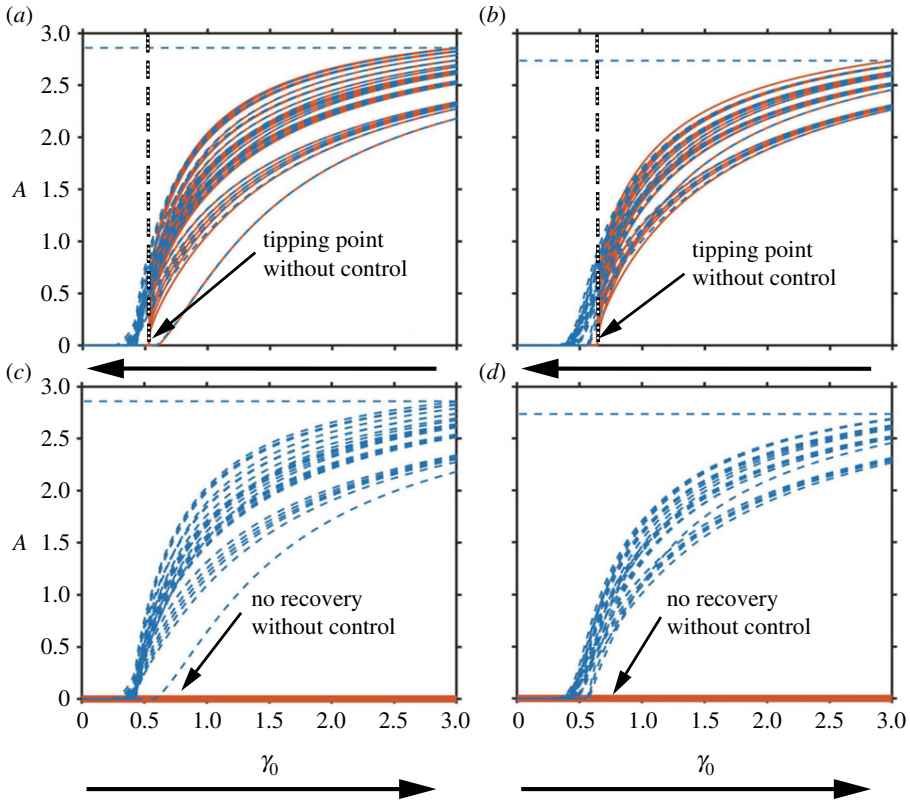

Figure 2. Tipping points in mutualistic networks and the role of abundance management with different parameters. (*a*,*b*) In the absence of abundance management (brown curves), the occurrence of a tipping point for networks *A* and *B*, respectively, as the bifurcation parameter γ_0 is decreased through a critical point. Regardless of whether abundance management is absent or present, global extinction is inevitable (light blue dashed curves). The difference is that the extinction event is abrupt without abundance management but it becomes gradual with management (insets). (*c*,*d*) When the direction of change in γ_0 is reversed, species recovery is not possible without abundance management (the thick brown lines at $A \approx 0$). Controlled management enables a full recovery of all species once the value of γ_0 becomes larger than that associated with global extinction. The parameter values are $h = 0.3$, $t = 0.5$, $\beta_{ii}^{(A)} = \beta_{ii}^{(P)} = 1$, $\beta_{ij}^{(A)} = \beta_{ij}^{(P)} = 0$, $\alpha_i^{(A)} = \alpha_i^{(P)} = -0.1$, $\kappa_i = 0$ and $\mu_A = \mu_P = 0.0001$. (Online version in colour.)

3.3. Management strategy 1: maintaining the abundance of an influential pollinator

This is the same strategy discussed above for the case of varying the mutualistic interaction strength γ_0. As a result of management, plants connected to the controlled pollinator experience a growth in their population, elevating the equilibrium abundances, which in turn leads to a growth of the pollinators connected to those plants, and so on. This generates a positive feedback loop in the system. Suppose there are environmental changes so that the parameter κ increases slowly, rendering inevitable eventual collapse of the system. Inducing the positive feedback loop will delay the community collapse in the sense that the catastrophe associated with a tipping point can be changed into a gradual extinction process for larger values of κ. Figure 3*a* shows that, for network *A* under management, the pollinators become extinct at different values of κ, in contrast to the phenomenon of massive community collapse at the tipping point. The management strategy, in spite of its simplicity, can delay the event of total extinction. This result holds also for network *B*, as shown in figure 3*b*.

How will the system recover from a state in which the populations are near zero if the environment is improved so that κ is gradually decreased? Figure 3*c* shows, for network *A*, the recovery process from a state in which the pollinator abundance is only 0.01, for the two cases, i.e. with or without control. We see that, for the unmanaged system, there is a hysteresis phenomenon, where the value of κ required for the populations to fully recover is smaller than the tipping point value. This is a typical nonlinear hysteresis with the implication that it takes 'more' (in the sense that a smaller value κ is needed) for the system to recover once it has been in a state of near extinction. Since κ characterizes the environmental influence on the system, simply restoring the environment to a level preceding the collapse is not enough. Because of the emergence of the hysteresis loop, the environment needs to be more improved to restore the population abundances. Strikingly, when abundance management is present, the hysteresis effect has essentially disappeared (or is much weaker than that for the uncontrolled case). The significance is that proper management can greatly facilitate recovery of the ecosystem once it has evolved due to environmental deterioration to a state near total extinction. Similar behaviours occur for network *B*, as shown in figure 3*d*.

3.4. Management strategy 2: keeping the decay rate of an influential pollinator at zero

By this strategy, we target the pollinator that has the largest number of mutualistic connections to remove any factor contributing to its decay in abundance by setting its decay parameter to be zero. For other pollinators in the network, their decay parameter (κ) values are assumed to be identical

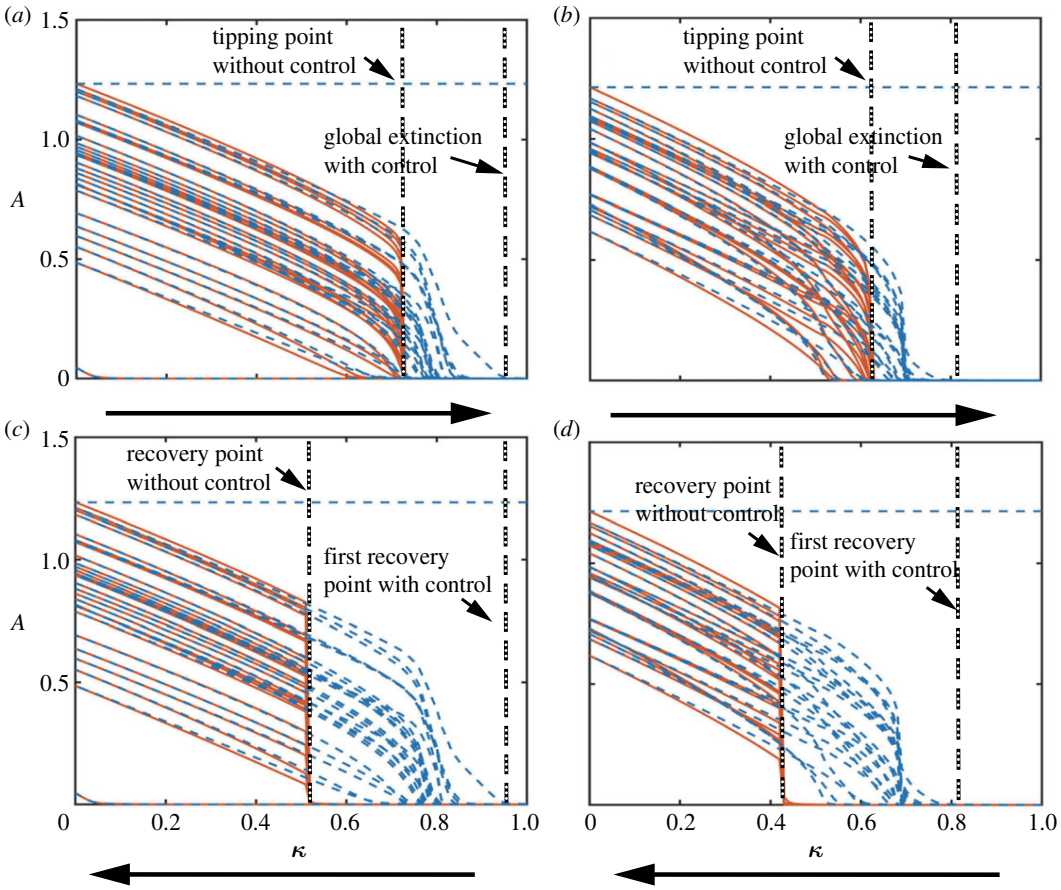

Figure 3. Managing a tipping point caused by an increase in the pollinator decay rate. The management principle is to maintain the abundance of the pollinator with the largest number of mutualistic connections (the horizontal light blue dashed line). Panels (*a*,*b*) show the delayed occurrence of total extinction as a result of abundance management for networks *A* and *B* described in the text, respectively. As the environment deteriorates (i.e. as κ is increased gradually), without abundance management, all pollinator populations collapse abruptly at a single value of κ—a tipping point. However, with abundance management, the extinction process becomes gradual, effectively removing the tipping point. In addition, the value of κ at which total extinction occurs is larger than that associated with the tipping point in the absence of abundance management. Panels (*c*,*d*) show the recovery dynamics for network *A* and *B*, respectively. Without abundance management, a hysteresis phenomenon arises, in which the value of κ required for a full population recovery is much smaller than that at the tipping point, stipulating that the environment needs to be much more improved than that preceding the collapse in order to restore the pollinator populations. The abundance management removes the hysteresis effect. The arrows indicate the respective directions of variation in κ. Simulation parameters are $\alpha = 0.15$, $\beta_{ii} = 1$, $\beta_{ij} = 0.01$, $\gamma_0 = 1$, $t = 0.5$, $h = 0.4$ and $\mu = 0.0001$. (Online version in colour.)

and can change due to environmental influences. As κ is increased toward a tipping point, we find that the abundance of the managed pollinator species can increase slightly while those of the other (uncontrolled) pollinator species decrease, a behaviour that can be attributed to interspecific competitions. In particular, as the value of κ is increased, the abundances of the unmanaged pollinators will decrease, leading to a reduction in interspecific competition for the managed pollinator species. As a result, the abundance of the managed pollinator species tends to increase, as exemplified in figure 4*a* for network *A*. The end result of the decay rate management can also be seen: it has removed the tipping point and delayed the occurrence of global extinction of the whole network system. A similar phenomenon occurs for network *B*, as shown in figure 4*b*. The dynamical behaviours of the system in response to environmental restoration, i.e. with a gradual decrease in κ, with or without decay rate management, are shown in figure 4*c*,*d* for networks *A* and *B*, respectively. Comparing figure 4*a*,*c*, we see that, for network *A*, without decay rate management, a hysteresis phenomenon similar to that in figure 3 (management strategy 1) arises, which disappears essentially when management is activated. A similar behaviour occurs for network *B*, as shown in figure 4*b*,*d*.

3.5. Controllability ranking of pollinators

The two strategies tested are to manage the pollinator with the largest number of mutualistic connections. We see that the management can have three effects: avoiding massive collapse of the abundances of all species, delaying the occurrence of global extinction and facilitating recovery of species. Maintaining the abundance of a different pollinator species may not have all the benefits. For example, targeting a pollinator species that does not possess the largest number of connections may not significantly mitigate the collapse of species. However, we find that the delay in the occurrence of the global extinction is a common feature, regardless of the particular pollinator species managed. It is thus useful to rank the controllability of the individual pollinator species in terms of the amount of management-induced delay in the critical value of the decay parameter κ.

We use network *B* and management strategy 2 to demonstrate the controllability ranking for the pollinator species. To

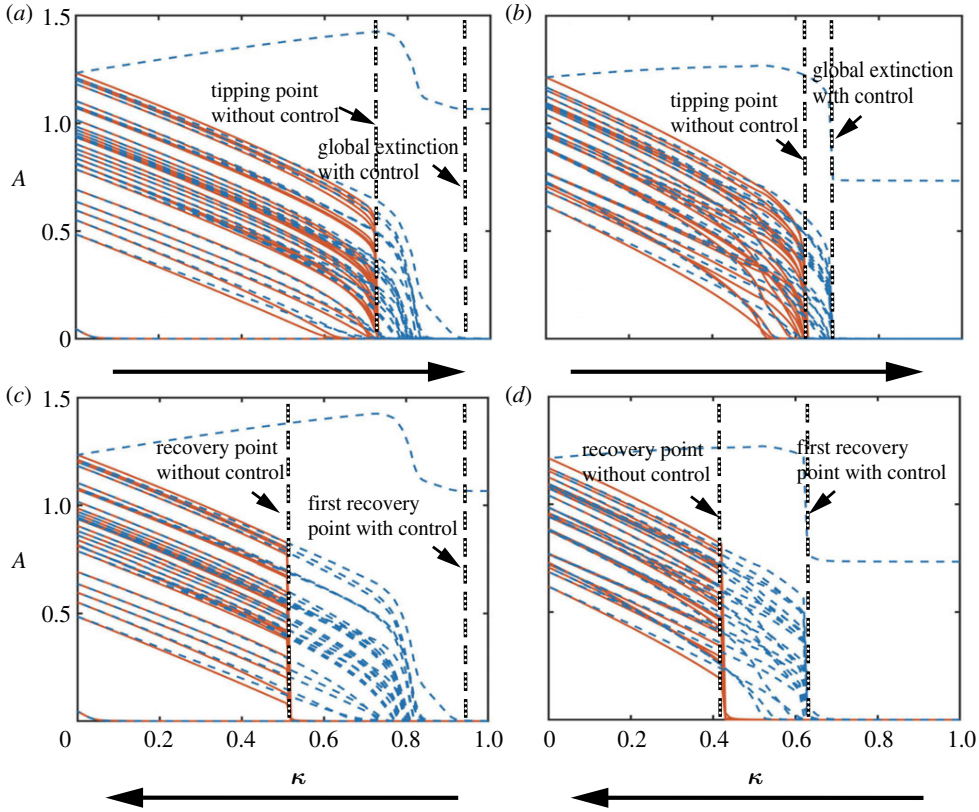

Figure 4. Managing a tipping point caused by an increase in the pollinator decay rate through an alternative strategy. The strategy entails making zero the decay rate of the pollinator with the largest number of mutualistic links. Panels (*a*,*b*) show the occurrence of a tipping point as the average decay parameter κ for all other pollinators is increased due to continuous deterioration of the environment, for networks *A* and *B*, respectively. Panels (*c*,*d*) show the steady-state species abundances versus κ for the opposite situation where the environment is gradually improved, for networks *A* and *B*, respectively. Similar to the results in figure 3, without decay rate management, a hysteresis loop emerges in that the value of κ needs to be smaller (corresponding to a more improved environment) in order to restore the pollinator abundances to the level before the tipping point. The decay rate management effectively removes the hysteresis. Simulation parameters are $\alpha = 0.15$, $\beta_{ii} = 1$, $\beta_{ij} = 0.01$, $\gamma_0 = 1$, $t = 0.5$, $h = 0.4$ and $\mu = 0.0001$. (Online version in colour.)

calculate the rank of the *i*th pollinator species, we examine the tipping point of the system in the absence of decay rate management and the critical value of global extinction in the presence of decay rate management. The absolute difference $\delta\kappa$ between the two critical values is a measure of the effectiveness of managing the *i*th pollinator. Figure 5*a–d* shows the delay $\delta\kappa$ resulting from managing four different pollinator species: 2, 3, 5 and 8, respectively. Pollinators 2 and 3 have the same number of interactions, but their values of delay $\delta\kappa$ are quite different. Managing pollinator species 5 and 8 gives a similar behaviour. For example, pollinator species 5 has the lowest abundance among the four species, and the corresponding value of $\delta\kappa$ is the smallest. Insights into the correlation exemplified in figure 5*a–d* can be gained from the network structure shown in fig. 2*d* in [18], where pollinator species 2 has a mutualistic interaction with plant species 2 but not with plant species 1. Pollinator species 3 has four mutualistic interactions, which include plant species 1 and 2. Pollinator species 5 has neither interaction with plant species 1 nor any with plant species 2, so it has the smallest value of $\delta\kappa$. In general, we anticipate that the connecting topology of the mutualistic network will have a dominant effect on the controllability ranking of the pollinators.

A surprising finding is that the network structure completely determines the controllability ranking of the pollinators. In particular, the ranking is determined the eigenvector V of the largest eigenvalue of the projection network M_p. Let M be the $m \times n$ matrix characterizing the structure of the bipartite network with m pollinators and n plant species. The projection network of the pollinators is characterized by $M_p = M \cdot M^T$. Figure 5*e* shows the numerically determined controllability ranking for the whole network versus the component value of the eigenvector V. There is a high degree of linear correlation between the two quantities.

4. Analysis

We have developed an approximate theory to understand the phenomenon of abundance control or management enabled recovery in mutualistic networks with a tipping point. In particular, given a network, we aim to predict the critical point γ_0^c at which species recovery begins as enabled by management. The basic idea is that the abrupt transition at a tipping point is one by which the system switches from a survival state (a high stable steady state, HSSS) to an extinction state (a low stable steady state, LSSS), and the reverse transition occurs at a recovery point. Bistability is characteristic of nonlinear dynamical systems with a tipping point. Between the LSSS and HSSS, there is an unstable steady state (USS). Recovery from the LSSS occurs when certain species abundances exceed the value in the USS. The key to predicting the recovery point lies thus in finding the USS.

The starting point of our mathematical analysis of the resilience functions of complex mutualistic networks is to modify the recently developed two-dimensional reduced

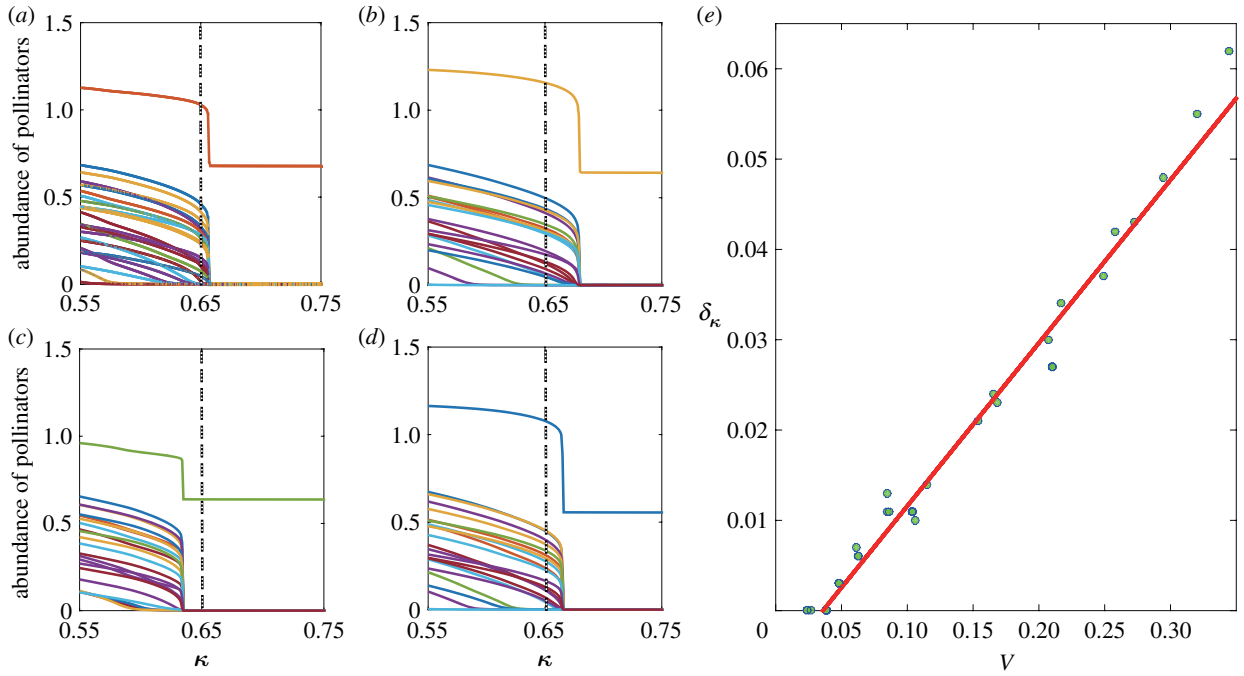

Figure 5. Controllability ranking of pollinators. (*a–d*) For network *B*, the delay in the critical decay parameter for global extinction, $\delta\kappa$, resulting from controlling pollinators 2, 3, 5 and 8, respectively (see fig. 2*d* in [18]). The vertical dashed lines at $\kappa = 0.65$ are for eye guidance. (*e*) Controllability ranking according to $\delta\kappa$, where the pollinators are ordered in terms of *V*, the eigenvector of the largest eigenvalue of the projection matrix M_p of the bipartite network. (Online version in colour.)

model for these networks [18], taking into account the effect of abundance control management. The original reduced model [18] is

$$\frac{dP_e}{dt} = \alpha P_e - \beta P_e^2 + \frac{(\langle\gamma_P\rangle A_e)}{(1+h\langle\gamma_P\rangle A_e)}P_e + \mu \quad \text{and}$$
$$\frac{dA_e}{dt} = \alpha A_e - \beta A_e^2 + \frac{(\langle\gamma_A\rangle P_e)}{(1+h\langle\gamma_A\rangle P_e)}A_e + \mu, \tag{4.1}$$

where A_e and P_e are the properly averaged pollinator and plant abundances, respectively, α, β, $\langle\gamma_P\rangle$, $\langle\gamma_A\rangle$ and μ are the corresponding average parameters. In the original model [18], all pollinators are treated on equal footing, so are the plants. However, when control is present, the plant species directly connected to the managed pollinator species, the single pollinator species whose abundance is maintained externally, are distinct from other plant species. It is then necessary to remove the controlled pollinator species from the averaging process, but it affects the plant species that are directly connected to it. As a result, the values of the average mutualistic interaction parameters, $\langle\gamma_P\rangle$ and $\langle\gamma_A\rangle$, are modified. The eigenvector weighted averaging method [18] can be used to calculate these parameters (electronic supplementary material, Section IV). The steady-state solution of the ensemble averaged pollinator abundance A' in the presence of abundance management can be obtained through the quadratic equation

$$q_1 A'^2 + q_2 A' + q_3 = 0, \tag{4.2}$$

where the coefficients are given by

$$q_1 = -(\beta^2 h\langle\gamma_P\rangle + \beta h\langle\gamma_A\rangle\langle\gamma_P\rangle + \beta h^2\alpha\langle\gamma_A\rangle\langle\gamma_P\rangle),$$
$$q_2 = -\beta^2 - h\alpha\beta\langle\gamma_A\rangle + h\alpha\beta\langle\gamma_P\rangle + \langle\gamma_A\rangle\langle\gamma_P\rangle + 2h\alpha\langle\gamma_A\rangle\langle\gamma_P\rangle + h^2\alpha^2\langle\gamma_A\rangle\langle\gamma_p\rangle,$$
and $$q_3 = \alpha\beta + \alpha\langle\gamma_A\rangle + h\alpha^2\langle\gamma_A\rangle$$

The USS of the approximate ensemble averaged pollinator abundance is given by (electronic supplementary material, Section V)

$$A_{uss} = (-q_2 + \sqrt{q_2^2 - 4q_1q_3})/(2q_1).$$

The steady-state value of the ensemble averaged plant abundance can be obtained accordingly:

$$P_{uss} = \alpha + (\langle\gamma_P\rangle A_{uss})/(1 + h\langle\gamma_P\rangle A_{uss}),$$

which depends on the value of the bifurcation parameter γ_0.

Suppose the system is in the extinction state that satisfies $dP_i/dt = 0$ and $dA_i/dt = 0$, for $\gamma_0 \gtrapprox 0$, where $P_i \gtrapprox 0$ and $A_i \gtrapprox 0$. The steady-state plant and pollinator abundances are determined by

$$\alpha_i^{(P)} - \sum_{j=1}^{S_P}\beta_{ij}^{(P)}P_j + \left(\sum_{k=1}^{S_A}\gamma_{ik}^{(P)}A_k\right)\Big/\left(1 + h\sum_{k=1}^{S_A}\gamma_{ik}^{(P)}A_k\right) = -\mu_P/P_i$$

and

$$\alpha_i^{(A)} - \sum_{j=1}^{S_A}\beta_{ij}^{(A)}A_j + \left(\sum_{k=1}^{S_P}\gamma_{ik}^{(A)}P_k\right)\Big/\left(1 + h\sum_{k=1}^{S_P}\gamma_{ik}^{(A)}P_k\right) = -\mu_A/A_i.$$

As the value of γ_0 is increased, the abundances of the plant species directly connected to the managed pollinator species will increase. Among those plant species, for the one with the largest abundance, we have $\mu_P/P_i \approx 0$. For $\beta_{ii} = 1$ and $\beta_{ij} = 0$, the steady-state abundance of this plant species is given by

$$P_i \approx \alpha_i^{(p)} + [(\gamma_0/d_i)A_S]/(1 + h(\gamma_0/d_i)A_S),$$

where d_i is the number of pollinator species that this plant species is connected to. Let P_{max} be the maximum abundance of this plant species and let A_S be the constant abundance value of the controlled pollinator species. The criterion for recovery from extinction is $P_{max} \gtrsim P_{uss}$, from which the critical recovery point γ_0^c can be determined for a given value

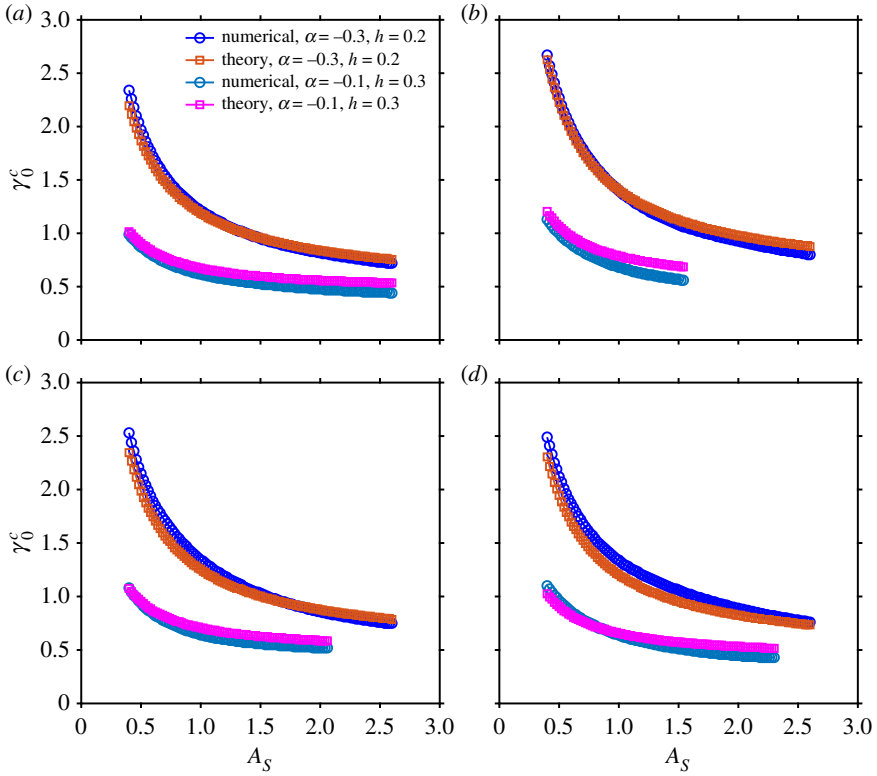

Figure 6. Predicted and numerically calculated recovery point as enabled by abundance management. (*a–d*) For networks *A–D*, respectively, the predicted (brown and magenta squares) and numerical (dark blue and light blue circles) species recovery point versus the constant abundance value A_S of the managed pollinator species with the largest degree. Other parameters are the same as those in figures 1 and 2. The light blue and magenta curves in (*b–d*) are shorter than the dark blue and brown curves because of the difficulty in determining accurately the recovery point for large values of the managed abundance A_S. (Online version in colour.)

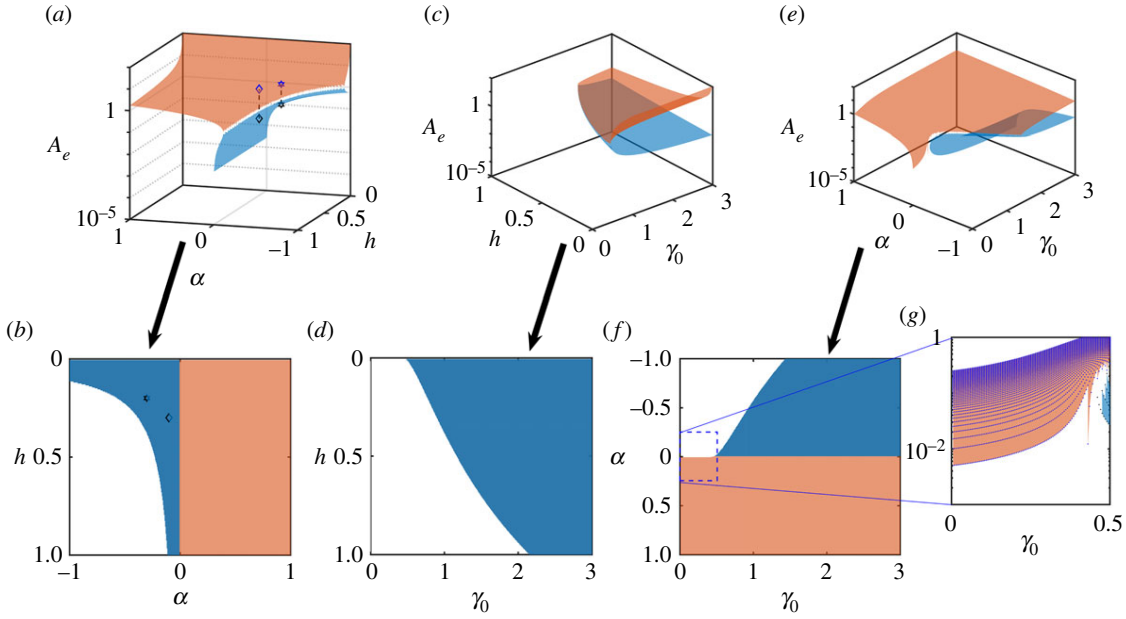

Figure 7. Stable and unstable steady states of the reduced model in the absence of management. Shown are the HSSS and USS for network *B* as represented by the brown and light blue surfaces, respectively, which are calculated from equation (4.2). (*a,b*) The effective pollinator abundance from the reduced model in the parameter planes: (*a,b*) (α, h) for $\gamma_0 = 1$, (*c,d*) (γ_0, h) for $\alpha = -0.3$, and (*e–g*) (γ_0, α) for $h = 0.2$, where (*g*) is an enlargement of the region $\alpha \in [-0.25, 0.25]$ and $\gamma_0 \in (0, 0.5]$ in (*f*). Other parameters are $t = 0.5$, $\mu = 0.0001$, and $\beta = 1.0$. Panels (*b,d,f*) are the bottom views of (*a,c,e*), respectively. In (*a,b*), the hexagon and diamond markers represent the HSSS and USS of the reduced model for the parameter settings in figures 1 and 2, respectively. In all panels, the pollinator abundance A_e is represented on a logarithmic scale. The plant abundance P_e is calculated from $P_e = \alpha + (\langle\gamma_P\rangle A_e)/(1 + h\langle\gamma_P\rangle A_e)$. (Online version in colour.)

of A_S. We emphasize that using a relatively large value A_S will make the tipping and recovery points coincide with each other. Figure 6*a–d* shows, for networks *A–D*, respectively, that the predicted recovery point versus A_S agrees remarkably well with that from direct numerical simulations of the original networks. A statistical analysis of the

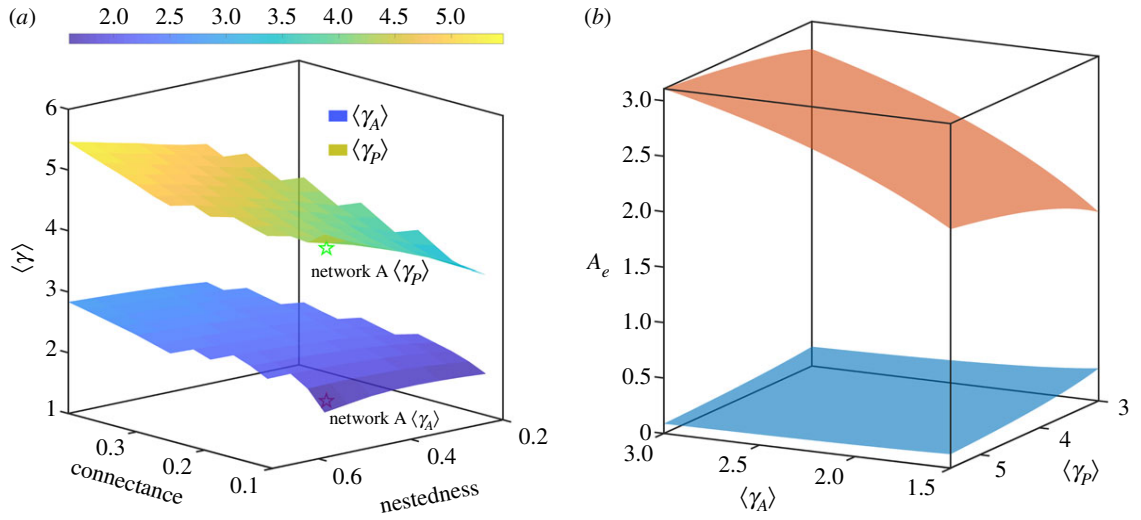

Figure 8. Effects of network structure on tipping point management. (*a*) The average species abundances $\langle \gamma_A \rangle$ (blue) and $\langle \gamma_P \rangle$ (green) for an ensemble of 'artificial' mutualistic networks with different computationally realizable values of connectance and nestedness, where the numbers of the pollinator and plant species are the same as those for network *A*. For each network with specific connectance and nestedness values, the average quantities $\langle \gamma_A \rangle$ and $\langle \gamma_P \rangle$ are calculated from 100 independent network realizations. (*b*) From the reduced model, the HSSS (brown) and USS (light blue) values versus $\langle \gamma_A \rangle$ and $\langle \gamma_P \rangle$. The ranges of $\langle \gamma_A \rangle$ and $\langle \gamma_P \rangle$ are the same as those in (*a*). Other parameters are $\alpha = -0.3$, $h = 0.2$, $t = 0.5$, $\mu = 0.0001$ and $\beta = 1$. (Online version in colour.)

predictive power of the reduced model is presented in electronic supplementary material, Section VI.

The dynamical mechanism of abundance control or management enabled recovery in the aftermath of a tipping point transition is that certain species abundances exceed the value in the USS, triggering a recovery from the LSSS. The USS is thus key to species recovery. Figure 7 shows the quantity A_e of the reduced model with respect to variations in the three main parameters: γ_0, h and α. As indicated by figure 6, for systems at the small parameter setting as that in figure 2, recovery occurs at a much smaller value of γ_0^C than that in systems with parameter setting as that in figure 1. This is because, the smaller the value of α from the negative side, the closer the value of USS is to zero, as shown in figure 7*a*. In fact, the abundances of some species can readily exceed the USS value in the presence of abundance management if it is near zero, initiating a recovery. Figure 7*b* shows that positive USS values exist only when α becomes negative. For $\alpha = -0.3$, the tipping point as characterized by the value of γ_0 increasing with h. For $\alpha > 0$, the HSSS is the only abundance state that the system can be in. Figure 7*c*,*d* shows the tipping point predicted by the reduced model. Figure 7*f* shows the region (light blue) in which the USS has a positive value and recovery is enabled by abundance management. In figure 7*b*,*f*, $\alpha = 0$ is the critical point for the system to have a positive valued USS. Mathematically, this occurs because, for $\alpha = 0$, the quantity q_3 in equation (4.2) vanishes. For $\alpha > 0$, the USS value is negative because of the conditions $q_1 < 0$ and $q_3 > 0$. The reduced model thus indicates the absence of any tipping point for $\alpha > 0$. Figure 7*g* shows that, for $\alpha \gtrapprox 0$, gradual extinction of species one after another will occur as the value of γ_0 is decreased, leading to global extinction for $\gamma_0 \gtrapprox 0$. However, in this case, there is no tipping point. (Simulations of the original high-dimensional dynamical network reveal essentially the same result, as shown in Section II of electronic supplementary material.) The results in figure 7 thus provide strong support for the power of the reduced model. (In electronic supplementary material, Section III, we provide a stability analysis of the stable steady-state solutions of the reduced model.)

Taken together, for $\alpha < 0$, a tipping point can occur as the value of γ_0 is decreased. In this case, after the total collapse, with abundance management the system can be restored as the value of γ_0 is increased. Ecologically, this means that, when the intrinsic growth rates of the pollinator and plant species are negative, the whole mutualistic system will exhibit a tipping point as the average mutualistic strength is reduced. Species recovery is ruled out without abundance management, but controlled maintenance of the abundance of a single species will enable full recovery of all species in the networked system.

How does the structure of the mutualistic network, especially in terms of the measures of connectance and nestedness, affect abundance management? To address this question, we generate an ensemble of mutualistic networks with systematically varying connectance and nestedness values where, for each network, the numbers of the pollinator and plant species are the same as those of network *A*. Figure 8*a* shows that the value γ in the reduced model increases as the network becomes more connected and nested. For example, if the connectance value is 0.2, as the value of nestedness is increased from 0.2 to 0.6, the values of $\langle \gamma_P \rangle$ and $\langle \gamma_A \rangle$ increase from 3.561 to 4.507 and from 1.968 to 2.225, respectively. If we set the nestedness value to 0.45 and increase the connectance value from 0.125 to 0.4, the values of $\langle \gamma_P \rangle$ and $\langle \gamma_A \rangle$ increase from 4.176 to 5.012 and from 1.712 to 2.721, respectively. Note that, because the network has 60 pollinator and 17 plant species, the value of $\langle \gamma_P \rangle$ is larger than that of $\langle \gamma_A \rangle$. We find that the variations of the effective value of γ in the reduced model are smooth and relatively small. Figure 8*b* shows the HSSS and USS values from the reduced model. Note the relatively large separation between the two values: the USS value is close to zero while the HSSS value is larger than one. The HSSS and USS values reach the maximum and minimum, respectively, when both values of $\langle \gamma_A \rangle$ and $\langle \gamma_P \rangle$ reach a maximum. This implies that an increase in the nestedness and connectance values will increase the HSSS value but reduce the USS value, facilitating control enabled species recovery. Regardless of the changes in the structure of the mutualistic

network, the phenomenon of abundance control or management enabled species recovery, as established by a dynamical analysis of the reduced model, persists.

In electronic supplementary material, Section I, we address additional issues pertinent to management, such as the effects of controlled abundance level on species recovery. The electronic supplementary material also treats the steady states in the reduced model and their stabilities with parameter variations.

5. Discussion

We emphasize the importance of taking into account biological constraints when formulating strategies to manage or control tipping points. Guided by this general principle, for complex mutualistic networks in ecology, we have articulated and analysed a realistic management strategy targeting a single pollinator to maintain its abundance at a constant level, with the main benefit being the removal of the catastrophic tipping point behaviour and the enabling of species recovery that otherwise would not be possible. These striking phenomena are uncovered when the tipping point is caused by continuous weakening of the mutualistic interaction strength between the pollinator and plant species. Variations in other parameters, such as a continuous increase in their decay rate, can trigger a tipping point as well. In such cases, species recovery is possible even without abundance management, but targeted control can remove the tipping point and facilitate recovery.

Theoretically, we have demonstrated that the recovery point can be predicted through a reduced, two-dimensional model that is a generalized version of the previously reduced model [18], because of the presence of control management of abundance. It is common knowledge in nonlinear dynamics that the unstable steady state plays a critical role in the system dynamics after a saddle-node bifurcation. The purpose of our analysis is to show that, by examining the unstable steady state in the reduced model, one can predict the tipping point transition in the full model, demonstrating the predictive power of the reduced model. Such a reduced model should be particularly useful in ecological systems where imperfect knowledge of the system may be likely. We have also studied how the network structure affects the unstable steady state and the effect of abundance management. Especially, if the numbers of pollinator and plant species are fixed, the value of the unstable steady state increases as the connectance and nestedness of the underlying network are enhanced, up to a limit. We thus expect our management strategy to be effective for real mutualistic networked systems with varying structures.

The problem of developing management/control principles and strategies to eliminate tipping points in complex and nonlinear networked systems has broad implications [59,60]. For the mutualistic networks treated in this paper *per se*, our management strategy to maintain the abundance of certain pollinator species may be realized through the approach of injecting robotic pollinators [70] to expedite recovery [71–74]. This may help address the devastating problem of relatively sudden disappearances of bee colonies, which are happening currently all over the world.

Data accessibility. All data and computer codes are available from the authors upon request.

Authors' contributions. Y.-C.L. and A.H. conceived the project. J.J.J. performed computations and analysis. All analysed data. Y.-C.L. and J.J.J. wrote the paper.

Competing interests. The authors declare that they have no competing interests.

Funding. We would like to acknowledge support from the Vannevar Bush Faculty Fellowship programme sponsored by the Basic Research Office of the Assistant Secretary of Defense for Research and Engineering and funded by the Office of Naval Research through grant no. N00014-16-1-2828. A.H. was supported by National Science Foundation under grant no. DMS-1817124.

References

1. Gladwell M. 2000 *The tipping point: how little thinkgs can make a big difference*. New York, NY: Little, Brown and Company.
2. Rahmstorf S. 2002 Ocean circulation and climate during the past 120 000 years. *Nature* **419**, 207–214. (doi:10.1038/nature01090)
3. Scheffer M. 2004 *Ecology of shallow lakes*. Berlin, Germany: Springer Science & Business Media.
4. Scheffer M *et al.* 2009 Early-warning signals for critical transitions. *Nature* **461**, 53–59. (doi:10.1038/nature08227)
5. Scheffer M. 2010 Complex systems: foreseeing tipping points. *Nature* **467**, 411–412. (doi:10.1038/467411a)
6. Wysham DB, Hastings A. 2010 Regime shifts in ecological systems can occur with no warning. *Ecol. Lett.* **13**, 464–472. (doi:10.1111/j.1461-0248.2010.01439.x)
7. Drake JM, Griffen BD. 2010 Early warning signals of extinction in deteriorating environments. *Nature* **467**, 456–459. (doi:10.1038/nature09389)
8. Boettiger C, Hastings A. 2012 Quantifying limits to detection of early warning for critical transitions. *J. R. Soc. Interface* **9**, 2527–2539. (doi:10.1098/rsif.2012.0125)
9. Dai L, Vorselen D, Korolev KS, Gore J. 2012 Generic indicators for loss of resilience before a tipping point leading to population collapse. *Science* **336**, 1175–1177. (doi:10.1126/science.1219805)
10. Ashwin P, Wieczorek S, Vitolo R, Cox P. 2012 Tipping points in open systems: bifurcation, noise-induced and rate-dependent examples in the climate system. *Phil. Trans. R. Soc. A* **370**, 1166–1184. (doi:10.1098/rsta.2011.0306)
11. Lenton TM, Livina VN, Dakos V, van Nes EH, Scheffer M. 2012 Early warning of climate tipping points from critical slowing down: comparing methods to improve robustness. *Phil. Trans. R. Soc. A* **370**, 1185–1204. (doi:10.1098/rsta.2011.0304)
12. Barnosky AD *et al*. 2012 Approaching a state shift in earth's biosphere. *Nature* **486**, 52–58. (doi:10.1038/nature11018)
13. Boettiger C, Hastings A. 2013 Tipping points: from patterns to predictions. *Nature* **493**, 157–158. (doi:10.1038/493157a)
14. Tylianakis JM, Coux C. 2014 Tipping points in ecological networks. *Trends Plant Sci.* **19**, 281–283. (doi:10.1016/j.tplants.2014.03.006)
15. Lever JJ, Nes EH, Scheffer M, Bascompte J. 2014 The sudden collapse of pollinator communities. *Ecol. Lett.* **17**, 350–359. (doi:10.1111/ele.12236)
16. Lontzek TS, Cai Y-Y, Judd KL, Lenton TM. 2015 Stochastic integrated assessment of climate tipping points indicates the need for strict climate policy. *Nat. Clim. Change* **5**, 441–444. (doi:10.1038/nclimate2570)
17. Gualdia S, Tarziaa M, Zamponic F, Bouchaudd J-P. 2015 Tipping points in macroeconomic agent-based models. *J. Econ. Dyn. Control* **50**, 29–61. (doi:10.1016/j.jedc.2014.08.003)
18. Jiang J, Huang ZG, Seager TP, Lin W, Grebogi C, Hastings A, Lai YC. 2018 Predicting tipping points in mutualistic networks through dimension reduction.

Proc. Natl Acad. Sci. USA **115**, E639–E647. (doi:10.1073/pnas.1714958115)

19. Liu Y-Y, Slotine J-J, Barabási A-L. 2011 Controllability of complex networks. *Nature* **473**, 167–173. (doi:10.1038/nature10011)
20. Wang W-X, Ni X, Lai Y-C, Grebogi C. 2012 Optimizing controllability of complex networks by minimum structural perturbations. *Phys. Rev. E* **85**, 026115. (doi:10.1103/PhysRevE.85.026115)
21. Nacher JC, Akutsu T. 2012 Dominating scale-free networks with variable scaling exponent: heterogeneous networks are not difficult to control. *New J. Phys.* **14**, 073005. (doi:10.1088/1367-2630/14/7/073005)
22. Nepusz T, Vicsek T. 2012 Controlling edge dynamics in complex networks. *Nat. Phys.* **8**, 568–573. (doi:10.1038/nphys2327)
23. Yuan Z, Zhao C, Di Z, Wang W-X, Lai Y-C. 2013 Exact controllability of complex networks. *Nat. Commun.* **4**, 2447. (doi:10.1038/ncomms3447)
24. Delpini D, Battiston S, Riccaboni M, Gabbi G, Pammolli F, Caldarelli G. 2013 Evolution of controllability in interbank networks. *Sci. Rep.* **3**, 1626. (doi:10.1038/srep01626)
25. Nacher JC, Akutsu T. 2013 Structural controllability of unidirectional bipartite networks. *Sci. Rep.* **3**, 1647. (doi:10.1038/srep01647)
26. Menichetti G, Dall'Asta L, Bianconi G. 2014 Network controllability is determined by the density of low in-degree and out-degree nodes. *Phys. Rev. Lett.* **113**, 078701. (doi:10.1103/PhysRevLett.113.078701)
27. Ruths J, Ruths D. 2014 Control profiles of complex networks. *Science* **343**, 1373–1376. (doi:10.1126/science.1242063)
28. Wuchty S. 2014 Controllability in protein interaction networks. *Proc. Natl Acad. Sci. USA* **111**, 7156–7160. (doi:10.1073/pnas.1311231111)
29. Yuan Z-Z, Zhao C, Wang W-X, Di Z-R, Lai Y-C. 2014 Exact controllability of multiplex networks. *New J. Phys.* **16**, 103036. (doi:10.1088/1367-2630/16/10/103036)
30. Pasqualetti F, Zampieri S, Bullo F. 2014 Controllability metrics, limitations and algorithms for complex networks. *IEEE Trans. Control Netw. Syst.* **1**, 40–52. (doi:10.1109/TCNS.2014.2310254)
31. Xiao Y-D, Lao S-Y, Hou L-L, Bai L. 2014 Edge orientation for optimizing controllability of complex networks. *Phys. Rev. E* **90**, 042804. (doi:10.1103/PhysRevE.90.042804)
32. Sorrentino F. 2014 Effects of the network structural properties on its controllability. *Chaos* **17**, 033101. (doi:10.1063/1.2743098)
33. Wu F-X, Wu L, Wang J-X, Liu J, Chen L-N. 2014 Transittability of complex networks and its applications to regulatory biomolecular networks. *Sci. Rep.* **4**, 4819. (doi:0.1038/srep04819)
34. Whalen AJ, Brennan SN, Sauer TD, Schiff SJ. 2015 Observability and controllability of nonlinear networks: the role of symmetry. *Phys. Rev. X* **5**, 011005. (doi:10.1103/physrevx.5.011005)
35. Nacher JC, Akutsu T. 2015 Structurally robust control of complex networks. *Phys. Rev. E* **91**, 012826. (doi:10.1103/PhysRevE.91.012826)
36. Summers TH, Cortesi FL, Lygeros J. 2015 On submodularity and controllability in complex dynamical networks. *IEEE Trans. Control Netw. Syst.* **3**, 91–101. (doi:10.1109/TCNS.2015.2453711)
37. Iudice FL, Garofalo F, Sorrentino F. 2015 Structural permeability of complex networks to control signals. *Nat. Commun.* **6**, 8349. (doi:10.1038/ncomms9349)
38. Chen Y-Z, Wang L-Z, Wang W-X, Lai Y-C. 2016 Energy scaling and reduction in controlling complex networks. *R. Soc. open sci.* **3**, 160064. (doi:10.1098/rsos.160064)
39. Wang L-Z, Chen Y-Z, Wang W-X, Lai Y-C. 2017 Physical controllability of complex networks. *Sci. Rep.* **7**, 40198. (doi:10.1038/srep40198)
40. Klickstein I, Shirin A, Sorrentino F. 2017 Energy scaling of targeted optimal control of complex networks. *Nat. Commun.* **8**, 15145. (doi:10.1038/ncomms15145)
41. Wang XF, Chen G. 2002 Pinning control of scale-free dynamical networks. *Physica A* **310**, 521–531. (doi:10.1016/S0378-4371(02)00772-0)
42. Fiedler B, Mochizuki A, Kurosawa G, Saito D. 2013 Dynamics and control at feedback vertex sets. I: informative and determining nodes in regulatory networks. *J. Dyn. Differ. Equ.* **25**, 563–604. (doi:10.1007/s10884-013-9312-7)
43. Mochizuki A, Fiedler B, Kurosawa G, Saito D. 2013 Dynamics and control at feedback vertex sets. II: a faithful monitor to determine the diversity of molecular activities in regulatory networks. *J. Theor. Biol.* **335**, 130–146. (doi:10.1016/j.jtbi.2013.06.009)
44. Wells DK, Kath WL, Motter AE. 2015 Control of stochastic and induced switching in biophysical networks. *Phys. Rev. X* **5**, 031036. (doi:10.1103/physrevx.5.031036)
45. Wang L-Z, Su RQ, Huang ZG, Wang X, Wang WX, Grebogi C, Lai YC. 2016 A geometrical approach to control and controllability of nonlinear dynamical networks. *Nat. Commun.* **7**, 11323. (doi:10.1038/ncomms11323)
46. Zañudo JGT, Yang G, Albert R. 2017 Structure-based control of complex networks with nonlinear dynamics. *Proc. Natl Acad. Sci. USA* **114**, 7234–7239. (doi:10.1073/pnas.1617387114)
47. Klickstein I, Shirin A, Sorrentino F. 2017 Locally optimal control of complex networks. *Phys. Rev. Lett.* **119**, 268301. (doi:10.1103/PhysRevLett.119.268301)
48. Sun Y-Z, Leng S-Y, Lai Y-C, Grebogi C, Lin W. 2017 Closed-loop control of complex networks: a trade-off between time and energy. *Phys. Rev. Lett.* **119**, 198301. (doi:10.1103/PhysRevLett.119.198301)
49. Nishikawa T, Ott E. 2014 Controlling systems that drift through a tipping point. *Chaos* **24**, 033107. (doi:10.1063/1.4887275)
50. Vidiella B, Sardanyés J, Solé R. 2018 Exploiting delayed transitions to sustain semiarid ecosystems after catastrophic shifts. *J. R. Soc. Interface* **15**, 20180083. (doi:10.1098/rsif.2018.0083)
51. Bascompte J, Jordano P, Melián CJ, Olesen JM. 2003 The nested assembly of plant-animal mutualistic networks. *Proc. Natl Acad. Sci. USA* **100**, 9383–9387. (doi:10.1073/pnas.1633576100)
52. Guimaraes PR, Jordano P, Thompson JN. 2011 Evolution and coevolution in mutualistic networks. *Ecol. Lett.* **14**, 877–885. (doi:10.1111/j.1461-0248.2011.01649.x)
53. Nuismer SL, Jordano P, Bascompte J. 2013 Coevolution and the architecture of mutualistic networks. *Evolution* **67**, 338–354. (doi:10.1111/j.1558-5646.2012.01801.x)
54. Rohr RP, Saavedra S, Bascompte J. 2014 On the structural stability of mutualistic systems. *Science* **345**, 1253497. (doi:10.1126/science.1253497)
55. Dakos V, Bascompte J. 2014 Critical slowing down as early warning for the onset of collapse in mutualistic communities. *Proc. Natl Acad. Sci. USA* **111**, 17 546–17 551. (doi:10.1073/pnas.1406326111)
56. Guimaraes PR, Pires MM, Jordano P, Bascompte J, Thompson JN. 2017 Indirect effects drive coevolution in mutualistic networks. *Nature* **550**, 511–514. (doi:10.1038/nature24273)
57. Ohgushi T, Schmitz O, Holt RD. 2012 *Trait-mediated indirect interactions: ecological and evolutionary perspectives*. Cambridge, UK: Cambridge University Press.
58. Miller-Struttmann NE *et al*. 2015 Functional mismatch in a bumble bee pollination mutualism under climate change. *Science* **349**, 1541–1544. (doi:10.1126/science.aab0868)
59. Pace ML, Batt RD, Buelo CD, Carpenter SR, Cole JJ, Kurtzweil JT, Wilkinson GM. 2017 Reversal of a cyanobacterial bloom in response to early warnings. *Proc. Natl Acad. Sci. USA* **114**, 353–357. (doi:10.1073/pnas.1612424114)
60. Biggs R, Carpenter SR, Brock WA. 2009 Turning back from the brink: detecting an impending regime shift in time to avert it. *Proc. Natl Acad. Sci. USA* **106**, 826–831. (doi:10.1073/pnas.0811729106)
61. Gao J, Barzel B, Barabási A-L. 2016 Universal resilience patterns in complex networks. *Nature* **530**, 307–312. (doi:10.1038/nature16948)
62. Holling CS. 1959 Some characteristics of simple types of predation and parasitism. *Can. Entomol.* **91**, 385–398. (doi:10.4039/Ent91385-7)
63. Holling CS. 1973 Resilience and stability of ecological systems. *Annu. Rev. Ecol. Syst.* **4**, 1–23. (doi:10.1146/annurev.es.04.110173.000245)
64. Saavedra S, Rohr RP, Dakos V, Bascompte J. 2013 Estimating the tolerance of species to the effects of global environmental change. *Nat. Commun.* **4**, 2350. (doi:10.1038/ncomms3350)
65. Dicks L, Corbet S, Pywell R. 2002 Compartmentalization in plant–insect flower visitor webs. *J. Anim. Ecol.* **71**, 32–43. (doi:10.1046/j.0021-8790.2001.00572.x)
66. Montero AC. 2005 The ecology of three pollinator network. Master's thesis, Aarhus University, Aarhus, Denmark.
67. Dupont YL, Hansen DM, Olesen JM. 2003 Structure of a plant–flower-visitor network in the high-altitude sub-alpine desert of Tenerife, Canary Islands. *Ecography* **26**, 301–310. (doi:10.1034/j.1600-0587.2003.03443.x)
68. Motten AF. 1982 Pollination ecology of the spring wildflower community in the deciduous forests of piedmont North Carolina. PhD thesis, Duke University, Durham, NC, USA.

69. Traveset A, Richardson DM. 2014 Mutualistic interactions and biological invasions. *Annu. Rev. Ecol. Evol. Syst.* **45**, 89–113. (doi:10.1146/annurev-ecolsys-120213-091857)
70. Chechetka SA, Yu Y, Tange M, Miyako E. 2017 Materially engineered artificial pollinators. *Chemistry* **2**, 224–239. (doi:10.1016/j.chempr.2017.01.008)
71. Traveset A, Richardson DM. 2006 Biological invasions as disruptors of plant reproductive mutualisms. *Trends Ecol. Evol.* **21**, 208–216. (doi:10.1016/j.tree.2006.01.006)
72. Goulson D, Nicholls E, Botías C, Rotheray EL. 2015 Bee declines driven by combined stress from parasites, pesticides, and lack of flowers. *Science* **347**, 1255957. (doi:10.1126/science.1255957)
73. Rundlöf M *et al.* 2015 Seed coating with a neonicotinoid insecticide negatively affects wild bees. *Nature* **521**, 77–80. (doi:10.1038/nature14420)
74. Potts SG *et al.* 2016 Safeguarding pollinators and their values to human well-being. *Nature* **540**, 220–229. (doi:10.1038/nature20588)

Supplementary Information for

Harnessing tipping points in complex ecological networks

Junjie Jiang, Alan Hastings, and Ying-Cheng Lai

Corresponding author: Y.-C. Lai (Ying-Cheng.Lai@asu.edu)

Journal of the Royal Society Interface

CONTENTS

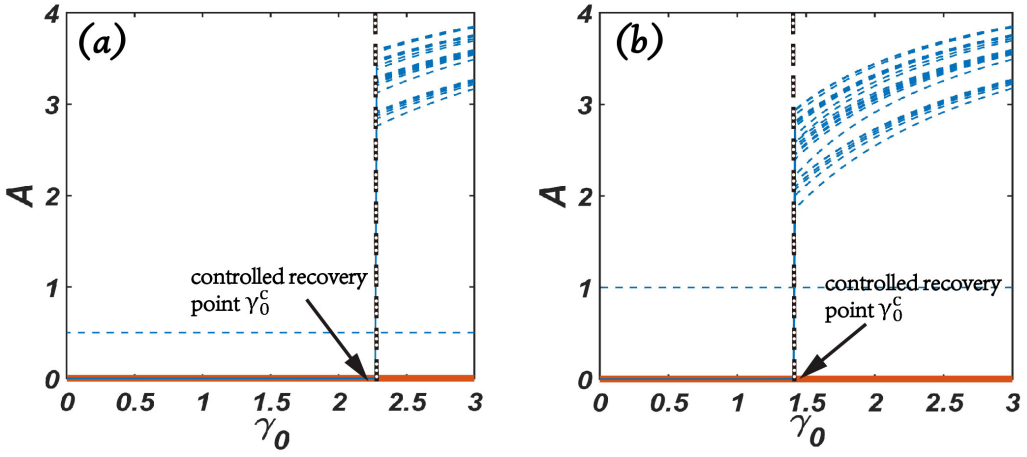

FIG. S1. **Effect of maintained abundance level of the target species on species recovery for a mutualistic network**. For network *B* described in the main text, for two different and relatively low values of the managed abundance of the target species (horizontal dashed line - these values should be compared with the corresponding value of about 4.0 in Fig. 1 in the main text): 0.5 for (a) and 1.0 for (b), successful recovery of all species as the average mutualistic interaction strength γ_0 is increased. Initially, the whole system is in an extinction state with near zero abundances. The data points plotted are the steady state abundance values of all the pollinator species. As predicted by the mathematical analysis in the main text, the level of maintained abundance does have an effect on the recovery point γ_0^c: a smaller value of the level leads to a larger value of γ_0^c. Without abundance management, species recovery is ruled out, as indicated by the thick blue lines at $A = 0$ for both panels. All other parameters have the same values as those in Fig. 1 in the main text.

I. EFFECT OF MAINTAINED ABUNDANCE LEVEL OF THE TARGET SPECIES ON RECOVERY

In Fig. 1 in the main text, the maintained abundance level of the target species for each pollinator-plant mutualistic network is set to a relatively high value. Figure S1 shows, for one of the networks, that a reduction in the level does not impede species recovery.

II. CONTINUOUS EXTINCTION AND RECOVERY PROCESSES IN THE REGIME OF WEAK INTRINSIC GROWTH

In Figs. 4(e-g) in the main text, the gradual extinction of species occurs in the regime when the intrinsic growth rate α of the pollinator species is positive and near zero. The dynamical analysis of the reduced model in the main text indicates that, when the value of α is decreased from a small positive to a negative value, the value of the HSSS moves continuously from the positive to the negative side. Thus, when the value of α is slightly positive, the species abundances gradually decrease to zero as the mutualistic interaction parameter γ_0 decreases to zero. Simulations of empirical networks reveal essentially the same behaviors, as illustrated in Fig. S2 for networks *A* and *B*, providing further support for the ability of the reduced model to capture the essential dynamical features of the high-dimensional mutualistic networks in the real world.

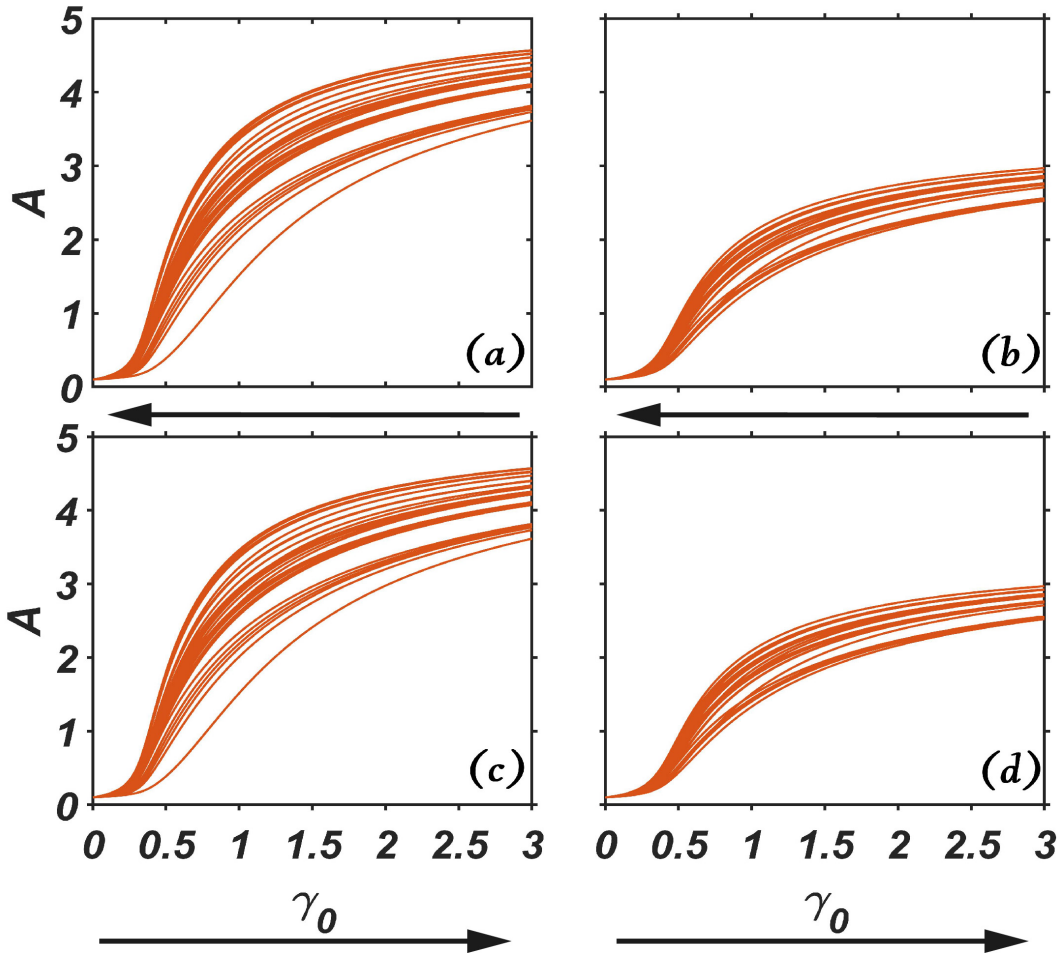

FIG. S2. *Species extinction and recovery as continuous processes in pollinator-plant mutualistic networks*. The systems illustrated are empirical networks A and B as described in the main text, and the continuous extinction and recovery processes occur in the regime of small and positive values of the intrinsic growth rate of the pollinator species. (a,b) In the absence of abundance management (brown curves), extinction of species occurs one after another in a "continuous" fashion for networks A and B, respectively, as the bifurcation parameter γ_0 is decreased from a relatively large value to zero. (c,d) When the value of γ_0 is increased from zero, each species recovers exactly at its point of extinction. The parameter values are $h = 0.2$, $t = 0.5$, $\beta_{ii}^{(A)} = \beta_{ii}^{(P)} = 1$, $\beta_{ij}^{(A)} = \beta_{ij}^{(P)} = 0$, $\alpha_i^{(A)} = \alpha_i^{(P)} = 0.1$, and $\mu_A = \mu_P = 0.0001$. The recovery dynamics can be predicted by the reduced model, as shown in Fig. 4(g) in the main text.

III. STABLE, UNSTABLE STEADY STATES AND THEIR STABILITY OF THE REDUCED MODEL WITH PARAMETER VARIATIONS

Figure S3 provides the results from a detailed stability analysis of the HSSS and USS of the reduced model constructed based on the parameters of the empirical network B in the main text. The eigenvalues of the HSSS are all negative, but the two eigenvalues of the USS have opposite signs, indicating that it is a saddle fixed point in the reduced two-dimensional system.

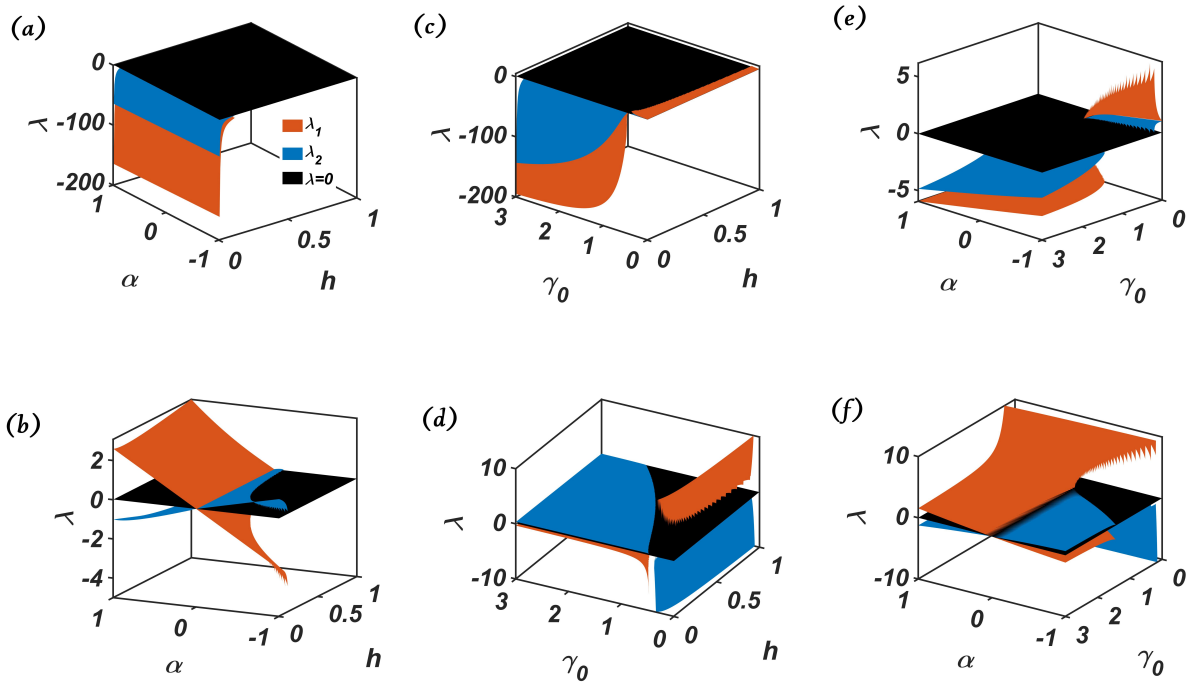

FIG. S3. *Stability of the steady states of the reduced model with parameter* γ_0 *and other parameters variation*. (a-f) The brown and light blue surfaces correspond to, respectively, the two eigenvalues of the Jacobian matrix evaluated at the steady states of the reduced model derived from network B based on Eq. (S5.12), where the black plane provides the zero value reference. Shown in different panels are the eigenvalues of HSSS and USS of the reduced model versus, respectively, (a,b) α and h for $\gamma_0 = 1$, (c,d) γ_0 and h for $\alpha = -0.3$, and (e,f) γ_0 and α for $h = 0.2$. Other parameter values are $t = 0.5$, $\mu = 0.0001$, and $\beta = 1$.

Because of the interspecific competitions in the empirical networks, it is necessary to use Eq. (S4.6) to calculate the effective intraspecific and interspecific competition rates. The steady state solutions of Eq. (S5.19) are given by

$$P' = \left[\alpha + \frac{\langle\gamma_P\rangle A'}{1+h\langle\gamma_P\rangle A'}\right]\beta_P^{-1}, \tag{S3.1}$$
$$A' = \left[\alpha - \kappa + \frac{\langle\gamma_A\rangle P'}{1+h\langle\gamma_A\rangle P'}\right]\beta_A^{-1},$$

and the algebraic equation of A' becomes

$$q_1 A'^2 + q_2 A' + q_3 = 0, \tag{S3.2}$$

where

$$\begin{aligned}
q_1 &= -(\beta_A\beta_P h\langle\gamma_P\rangle + \beta_A h\langle\gamma_A\rangle\langle\gamma_P\rangle + \beta_A h^2\alpha\langle\gamma_A\rangle\langle\gamma_P\rangle),\\
q_2 &= -\beta_A\beta_P - h\alpha\beta_A\langle\gamma_A\rangle + h\alpha\beta_P\langle\gamma_P\rangle + \langle\gamma_A\rangle\langle\gamma_P\rangle\\
&\quad +2h\alpha\langle\gamma_A\rangle\langle\gamma_P\rangle + h^2\alpha^2\langle\gamma_A\rangle\langle\gamma_P\rangle\\
&\quad -\kappa(h\beta_P\langle\gamma_P\rangle + h\langle\gamma_A\rangle\langle\gamma_P\rangle + h^2\alpha\langle\gamma_A\rangle\langle\gamma_P\rangle),\\
q_3 &= \alpha\beta_P + \alpha\langle\gamma_A\rangle + h\alpha^2\langle\gamma_A\rangle - \kappa(\beta_P + h\alpha\langle\gamma_A\rangle),
\end{aligned}$$

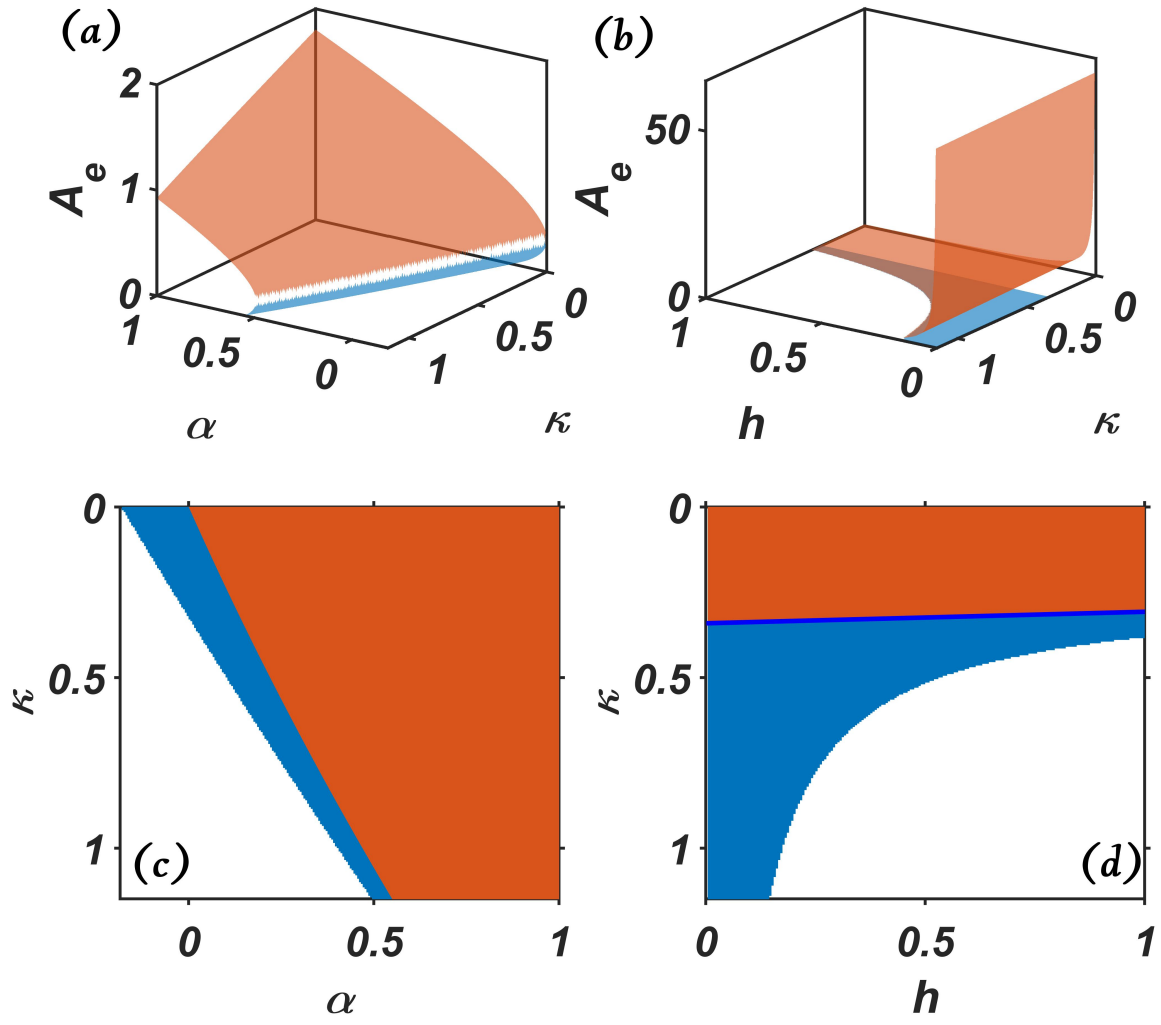

FIG. S4. *Stable and unstable steady states of the reduced model.* The reduced model is constructed based on the parameters of the empirical network B described in the main text, where the brown and light blue surfaces correspond to the HSSS and USS, respectively. Shown is the pollinator species abundance of the reduced model versus (a,c) α and κ for $h = 0.4$, and (b,d) h and κ for $\alpha = 0.15$. Other parameters are $t = 0.5$, $\mu = 0.0001$, and $\gamma 0 = 1$. Panels (c,d) are the bottom views of panels (a,b), respectively. The plant abundance can be obtained from the pollinator abundance according to the relation $P_e = \alpha + (\langle\gamma_P\rangle A_e)/(1 + h\langle\gamma_P\rangle A_e)$. In (d), the blue line indicates the movement of the USS from the positive to the negative side as the value of κ is decreased from one to zero.

Using the equation S3.2, we can calculate the HSSS and USS as shown in Fig. S4. The effective pollinator abundance A_e of the reduced model can explain why management can recover the mutualistic system and remove the hysteresis phenomenon. Figures S4(a-d) show that the HSSS and USS have positive values. In Fig. S4(b), The light blue region has positive HSSS and USS values, while in the brown region, HSSS is positive and USS is negative. In the white region, the HSSS and USS solutions are complex, which are ecologically not realistic. As shown in Fig. S4,the parameter region of α and κ with positive USS values is much smaller than that with positive HSSS

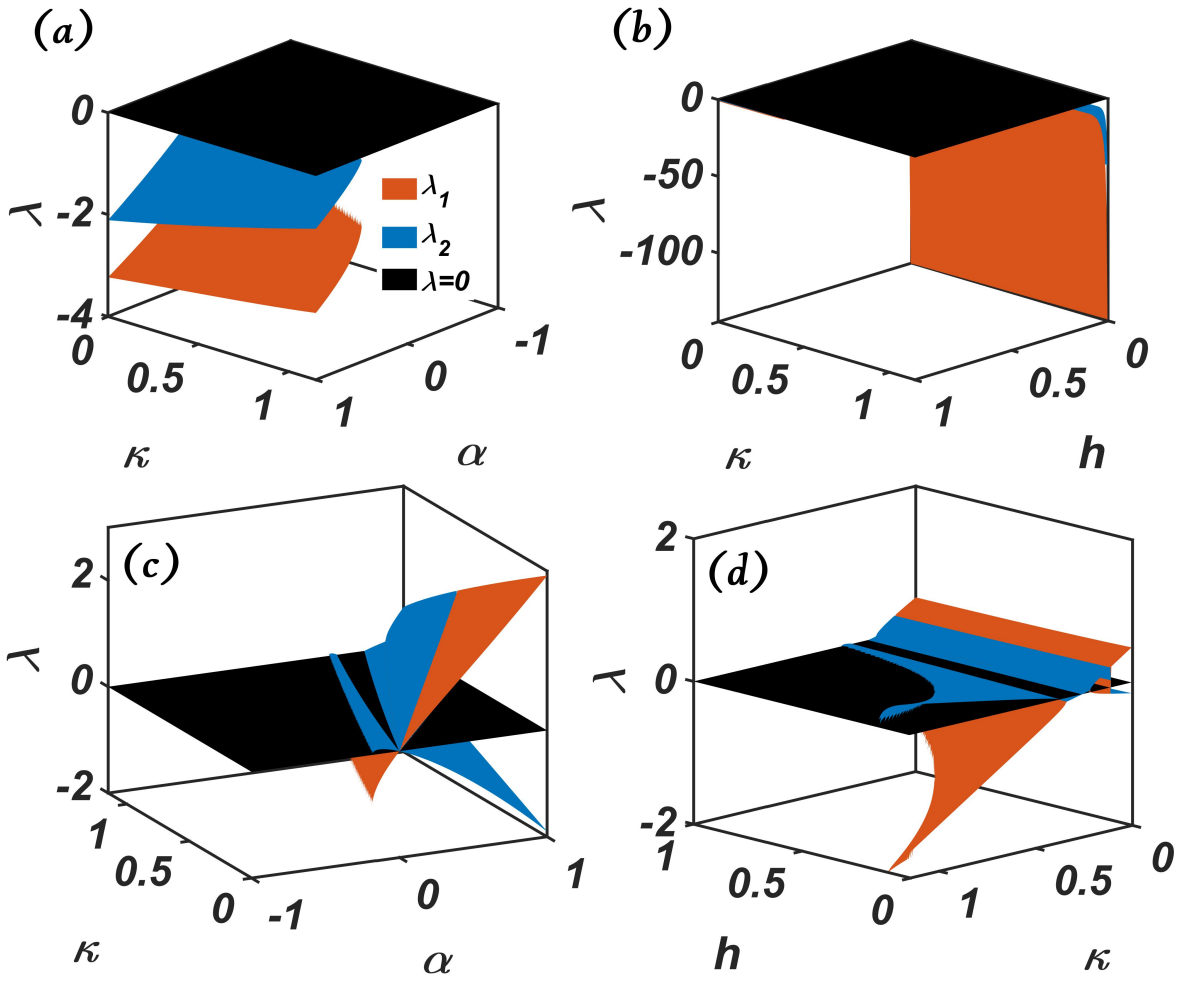

FIG. S5. *Stability of the steady states of the reduced model versus the pollinator decay rate* κ *and other parameters*. Shown are the two eigenvalues (brown and light blue surfaces) of the Jacobian matrix evaluated at the steady state of the reduced model constructed from the empirical network B. The eigenvalues of the HSSS and USS versus, respectively, (a,c) α and κ for $h = 0.4$, and (b,d) h and κfor $\alpha = 0.15$. Other parameters are $t = 0.5$, $\mu = 0.0001$, and $\gamma 0 = 1$.

values. As a result, when the value of κ is increased from zero to 1.15 for $\alpha \in [-0.185, 0.545]$, there exists a region with positive HSSS and USS values, and two transitions in κ: one separating the real from the complex USS solutions, and another separating the positive from the negative USS values. In Fig. S4(d), there are also three regions defined by two transitions. In all cases, a positively valued USS exists, indicating that controlled maintenance of a single, relatively large abundance pollinator species can recover the mutualistic system and remove the hysteresis in Fig.3 in main text.

The results of a stability analysis of the HSSS and USS solutions through the eigenvalues of the Jacobian matrix are presented in Fig. S5.

IV. DIMENSION REDUCTION FOR COMPLEX MUTUALISTIC NETWORKS SUBJECT TO CONTROL

In Ref. [1], an effective 2D model for arbitrary mutualistic networks in the absence of management was derived. Here we extend the dimension reduction approach to networks subject to abundance management. Some general considerations are the following. We assume there is a qualitative correspondence between the mutualistic interaction parameter γ_0 and the state of the environment in that a deteriorating environment for species leads to a decreased value of γ_0. As described in the main text, as γ_0 is decreased from a value at which the species abundances are stable and "healthy," a tipping point can occur at which the populations of all species collapse to near zero values, driving the system into extinction. As γ_0 is increased from a value associated with extinction, when abundance management is present, the system is able to recover. The recovery point is the critical value of γ_0 above which all species abundances have non-zero values. For simplicity, we also assume that the decay parameters for all the pollinators have an identical value: $\kappa_i \equiv \kappa$. There is a qualitative correspondence between κ and the state of the environment in that a deteriorating environment for species implies an increased value of κ. Increasing the value of κ can also lead to a tipping point.

Given a high-dimensional mutualistic network, the reduced dynamical system contains two coupled ODEs: one for all pollinator species except the one under management and another for the plant species. The basic idea of dimension reduction is to quantify the network structure by an effective parameter. The process consists of the following three steps.

We first obtain the effective (average) abundances of the plant and pollinator species. From Eq. (1) in the main text, we have

$$\alpha_i^{(P)} P_i \cong \alpha P_e \ \text{ and } \ \alpha_i^{(A)} A_i \cong \alpha A_e, \tag{S4.3}$$

where P_e and A_e are the effective abundances of the plant and the pollinator species, respectively. Secondly, since species do not out-compete each other when mutualistic partners are absent [2], intraspecific competitions are usually stronger than the interspecific competitions, leading to

$$\beta_{ii}^{(P)} \gg \beta_{ij}^{(P)} \ \text{ and } \ \beta_{ii}^{(A)} \gg \beta_{ij}^{(A)}. \tag{S4.4}$$

For simplicity, we neglect interspecific competitions. The terms describing species competitions in Eq. (1) in the main text can then be written as

$$\sum_{j=1}^{S_P} \beta_{ij}^{(P)} P_i P_j \approx \beta_{ii}^{(P)} P_i^2 \cong \beta P_e^2 \ \text{ and } \ \sum_{j=1}^{S_A} \beta_{ij}^{(A)} A_i A_j \approx \beta_{ii}^{(A)} A_i^2 \cong \beta A_e^2. \tag{S4.5}$$

However, the weak interspecific competitions can be taken into account by writing the species competition terms in Eq. (1) in the main text as

$$\sum_{j=1}^{S_P} \beta_{ij}^{(P)} P_i P_j \cong \frac{\sum_{i=1}^{S_P} \sum_{j=1}^{S_P} \beta_{ij}^{(P)}}{\sum_{i=1}^{S_P} 1} P_e^2 = \beta_P P_e^2 \ \text{ and } \ \sum_{j=1}^{S_A} \beta_{ij}^{(A)} A_i A_j \cong \frac{\sum_{i=1}^{S_A} \sum_{j=1}^{S_A} \beta_{ij}^{(A)}}{\sum_{i=1}^{S_A} 1} A_e^2 = \beta_A A_e^2. \tag{S4.6}$$

We treat the mutualistic strength for every single species:

$$\sum_{j=1}^{S_P}\gamma_{ij}^{(A)}P_j=\sum_{j=1}^{S_P}\frac{\gamma_0}{k_{A_i}^t}\varepsilon_{ij}P_j\cong\gamma_0 k_{A_i}^{(1-t)}P_e \text{ and } \sum_{j=1}^{S_A}\gamma_{ij}^{(P)}A_j=\sum_{j=1}^{S_A}\frac{\gamma_0}{k_{P_i}^t}\varepsilon_{ij}A_j\cong\gamma_0 k_{P_i}^{(1-t)}A_e, \tag{S4.7}$$

and calculate the average mutualistic interacting strength in the system through one of the following three averaging methods [1]: unweighted, degree weighting, and eigenvector weighting. Because of the complex topology of real-world mutualistic networks, we focus on the eigenvector weighting method. In particular, note that k_{P_i} and k_{A_i} are the numbers of the mutualistic interacting links associated with plant species P_i and pollinator species A_i, respectively. By the eigenvalue method, we calculate the averaging quantities for pollinator and plant species based on the eigenvector associated with the largest eigenvalue of the projection networks. Since abundance management is on to maintain the abundance of a single pollinator at a constant value, we exclude this species from the averaging process. Letting M_P and M_A be the projection matrices of the plants and pollinators, respectively, we have

$$M_P=M^T\times M,\ V_P=\text{eigenvector}(M_P) \text{ and } M_A=M\times M^T,\ V_A=\text{eigenvector}(M_A), \tag{S4.8}$$

where M is the $m\times n$ matrix characterizing the original bipartite network with m and n being the numbers of pollinator and plant species, V_P and V_A are the components of the eigenvector associated with the largest eigenvalue of M_P and M_A, respectively. We get

$$\langle\gamma_P\rangle=\frac{\sum_{i=1}^{S_P}\gamma_0 k_{P_i}^{1-t}\times V_P^{(i)}}{\sum_{i=1}^{S_A}V_P^{(i)}} \text{ and } \langle\gamma_A\rangle=\frac{\sum_{i=1}^{S_A}\gamma_0 k_{A_i}^{1-t}\times V_A^{(i)}}{\sum_{i=1}^{S_A}V_A^{(i)}}, \tag{S4.9}$$

where $V_P^{(i)}$ and $V_A^{(i)}$ are the i^{th} component of V_P and V_A, respectively. Let $\langle\gamma_P\rangle$ and $\langle\gamma_A\rangle$ be the effective mutualistic parameters for the plant and pollinator species in the absence of abundance management, respectively. Management will generate a change in these parameters:

$$\triangle\langle\gamma_P\rangle=\frac{\sum_{i=1}^{S_P}A_S\gamma_0 k_{P_i}^{-t}\times V_P^{(i)}}{\sum_{i=1}^{S_A}V_P^{(i)}} \tag{S4.10}$$

where A_S is the constant abundance value for the managed pollinator.

V. UNSTABLE STEADY STATE SOLUTION FOR PREDICTING THE RECOVERY POINT

The steady state solutions of the reduced model can be obtained by setting $dP_e/dt=0$ and $dA_e/dt=0$, which gives

$$f(P',A')=\alpha P'-\beta P'^2+\frac{\langle\gamma_P\rangle A'}{1+h\langle\gamma_P\rangle A'}P'+\mu=0, \tag{S5.11}$$
$$g(P',A')=\alpha A'-\beta A'^2+\frac{\langle\gamma_A\rangle P'}{1+h\langle\gamma_A\rangle P'}A'+\mu=0,$$

where A' and P' are the effective pollinator and plant abundances in the steady state, respectively. The Jacobian matrix associated with a steady-state solution is

$$J = \begin{bmatrix} \alpha - 2P'\beta + \frac{\langle\gamma_P\rangle A'}{1+h\langle\gamma_P\rangle A'} & -\frac{h\langle\gamma_P\rangle^2 A'P'}{(1+h\langle\gamma_P\rangle A')^2} + \frac{\langle\gamma_P\rangle P'}{1+h\langle\gamma_P\rangle A'} \\ -\frac{h\langle\gamma_A\rangle^2 A'P'}{(1+h\langle\gamma_A\rangle P')^2} + \frac{\langle\gamma_A\rangle A'}{1+h\langle\gamma_A\rangle P'} & \alpha - 2A'\beta - \kappa + \frac{\langle\gamma_A\rangle p'}{1+h\langle\gamma_A\rangle P'} \end{bmatrix}. \tag{S5.12}$$

The solutions of Eq. (S5.11) are

$$\begin{aligned} P' &= \frac{-(\alpha + \frac{\langle\gamma_P\rangle A'}{1+h\langle\gamma_P\rangle A'}) \pm [(\alpha + \frac{\langle\gamma_P\rangle A'}{1+h\langle\gamma_P\rangle A'})^2 + 4\beta\mu]^{1/2}}{-2\beta}, \\ A' &= \frac{-(\alpha - \kappa + \frac{\langle\gamma_A\rangle P'}{1+h\langle\gamma_A\rangle P'}) \pm [(\alpha - \kappa + \frac{\langle\gamma_A\rangle P'}{1+h\langle\gamma_A\rangle P'})^2 + 4\beta\mu]^{1/2}}{-2\beta}. \end{aligned} \tag{S5.13}$$

In general, we have $|\alpha| \gg \mu$. The physically meaningful solutions of A' and P' have positive values. We have $\beta\mu \ll |\alpha + \langle\gamma_P\rangle A'/(1+h\langle\gamma_P\rangle A')|$ or $|\alpha - \kappa + \langle\gamma_A\rangle P'/(1+h\langle\gamma_A\rangle P')|$. The approximate solutions of P' and A' are

$$\begin{aligned} P' &\approxeq \frac{-(\alpha + \frac{\langle\gamma_P\rangle A'}{1+h\langle\gamma_P\rangle A'}) \pm (|\alpha + \frac{\langle\gamma_P\rangle A'}{1+h\langle\gamma_P\rangle A'}| + 2\beta\mu)}{-2\beta}, \\ A' &\approxeq \frac{-(\alpha - \kappa + \frac{\langle\gamma_A\rangle P'}{1+h\langle\gamma_A\rangle P'}) \pm (|\alpha - \kappa + \frac{\langle\gamma_A\rangle P'}{1+h\langle\gamma_A\rangle P'}| + 2\beta\mu)}{-2\beta}. \end{aligned} \tag{S5.14}$$

For $\alpha + \langle\gamma_P\rangle A'/(1+h\langle\gamma_P\rangle A') > 0$, we have the following two approximate solutions of P':

$$\begin{aligned} P'_1 &\approxeq -\mu, \\ P'_2 &\approxeq \left[\alpha + \frac{\langle\gamma_P\rangle A'}{1+h\langle\gamma_P\rangle A'}\right]\beta^{-1}, \end{aligned} \tag{S5.15}$$

where P'_1 corresponds to the result in Eq. (S5.14) with the plus sign and P'_2 with the minus sign. Steady state solutions A'_1 and A'_2 can be obtained accordingly. For $\alpha + \langle\gamma_P\rangle A'/(1+h\langle\gamma_P\rangle A') < 0$, we have

$$\begin{aligned} P'_1 &\approxeq \left[\alpha + \frac{\langle\gamma_P\rangle A'}{1+h\langle\gamma_P\rangle A'}\right]\beta^{-1}, \\ P'_2 &\approxeq \mu. \end{aligned} \tag{S5.16}$$

For $\alpha - \kappa + \langle\gamma_A\rangle P'/(1+h\langle\gamma_A\rangle P') > 0$, we have

$$\begin{aligned} A'_1 &\approxeq -\mu, \\ A'_2 &\approxeq \left[\alpha - \kappa + \frac{\langle\gamma_A\rangle P'}{1+h\langle\gamma_A\rangle P'}\right]\beta^{-1}. \end{aligned} \tag{S5.17}$$

For $\alpha-\kappa+\langle\gamma_A\rangle P'/(1+h\langle\gamma_A\rangle P')<0$, we have

$$A_1' \approxeq \left[\alpha-\kappa+\frac{\langle\gamma_A\rangle P'}{1+h\langle\gamma_A\rangle P'}\right]\beta^{-1}, \tag{S5.18}$$
$$A_2' \approxeq \mu.$$

We consider the parameter regime in which the mutualistic system exhibits a tipping point. For initial state with high abundances, we have $\alpha-\kappa+\langle\gamma_A\rangle P'/(1+h\langle\gamma_A\rangle P')>0$ and $\alpha+\langle\gamma_P\rangle A'/(1+h\langle\gamma_P\rangle A')>0$, in the parameter region where the abundance values are relatively large, i.e., before the occurrence of a tipping point. In this case, the steady state solutions are given by Eqs. (S5.15) and (S5.17). The physically meaningful steady-state solutions are given by

$$P' = \left[\alpha+\frac{\langle\gamma_P\rangle A'}{1+h\langle\gamma_P\rangle A'}\right]\beta^{-1}, \tag{S5.19}$$
$$A' = \left[\alpha-\kappa+\frac{\langle\gamma_A\rangle P'}{1+h\langle\gamma_A\rangle P'}\right]\beta^{-1}.$$

The solution of Eq. (S5.19) can be conveniently expressed in terms of the following algebraic equation for A':

$$q_1 A'^2 + q_2 A' + q_3 = 0, \tag{S5.20}$$

where

$$\begin{aligned}
q_1 &= -(\beta^2 h\langle\gamma_P\rangle + \beta h\langle\gamma_A\rangle\langle\gamma_P\rangle + \beta h^2\alpha\langle\gamma_A\rangle\langle\gamma_P\rangle),\\
q_2 &= -\beta^2 - h\alpha\beta\langle\gamma_A\rangle + h\alpha\beta\langle\gamma_P\rangle + \langle\gamma_A\rangle\langle\gamma_P\rangle\\
&\quad +2h\alpha\langle\gamma_A\rangle\langle\gamma_P\rangle + h^2\alpha^2\langle\gamma_A\rangle\langle\gamma_p\rangle\\
&\quad -\kappa(h\beta\langle\gamma_P\rangle + h\langle\gamma_A\rangle\langle\gamma_P\rangle + h^2\alpha\langle\gamma_A\rangle\langle\gamma_P\rangle),\\
q_3 &= \alpha\beta + \alpha\langle\gamma_A\rangle + h\alpha^2\langle\gamma_A\rangle - \kappa(\beta + h\alpha\langle\gamma_A\rangle),
\end{aligned}$$

which gives a stable and an unstable solutions. Substituting the unstable solution of A' into Eq. (S5.19) yields the corresponding solution of P'.

VI. STATISTICAL ANALYSIS OF THE PREDICTIVE POWER OF THE REDUCED MODEL

To demonstrate the ability of the reduced model to predict the species recovery point in the presence of abundance management, we carry out a statistic analysis for different realizations of a random mutualistic network. The results are shown in Fig. S6. The process of generating independent statistical realizations of a mutualistic network is as follows. We first generate a random mutualistic network. We then use the nestedness algorithm [3] to increase the network's degree of nestedness. When the required nestedness is reached, we obtain the desired network. The predictive power of the reduced model can be characterized by the quantity $\delta\gamma$, the difference between the numerically calculated recovery point from the full system in the presence of abundance management and that predicted by the two-dimensional reduced model. In Fig. S6, the approximate values of the mean and standard deviation of the quantity $\delta\gamma$ for panels (a-d) are $(0.075, 0.080)$, $(0.031, 0.065)$, $(0.193, 0.090)$, and $(0.287, 0.073)$, respectively. In all cases, the statistical errors are approximately the same. The small mean values of $\delta\gamma$ in panels (a) and (b) indicate that the

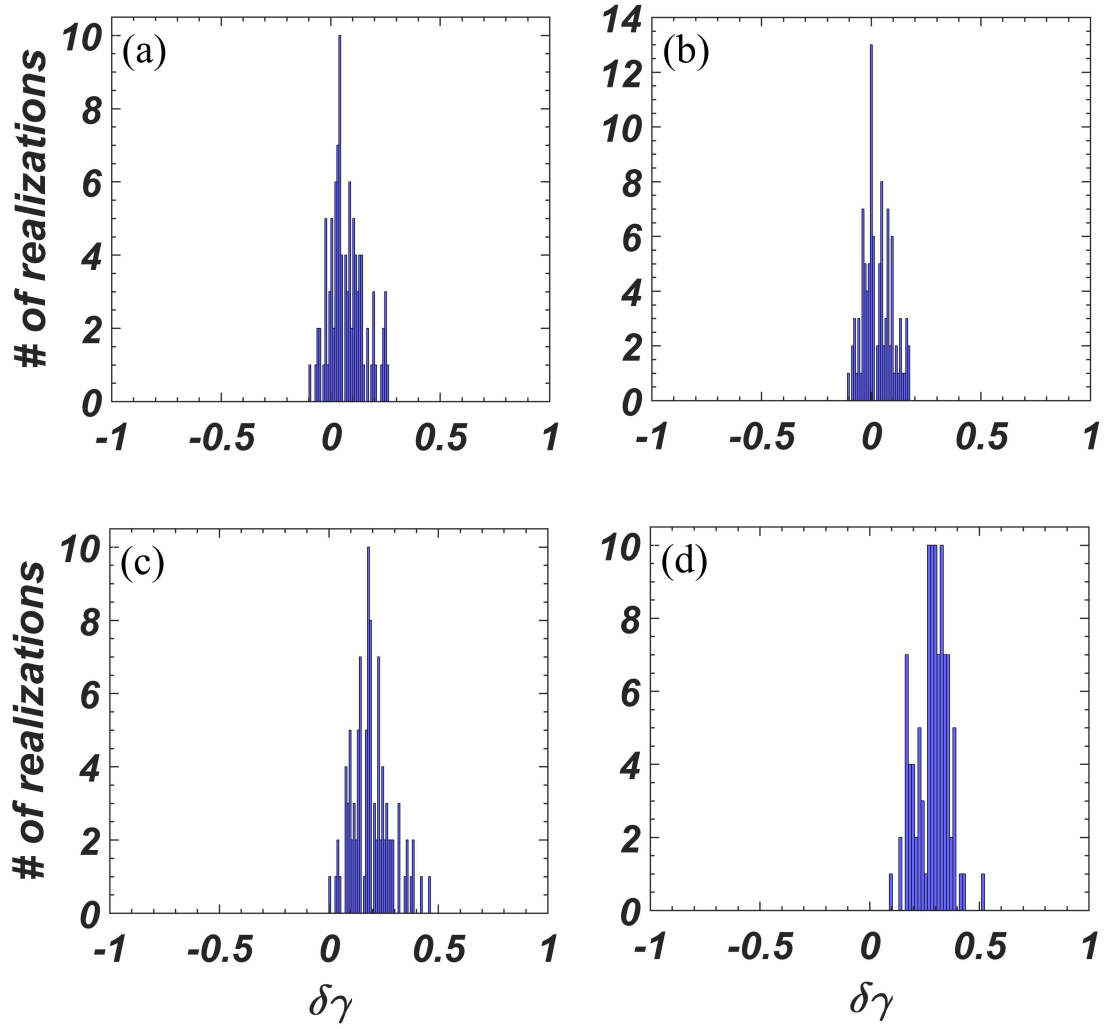

FIG. S6. *Statistical results on the ability of the reduced model to predict the species recovery point*. In all panels, the x-axis is $\delta\gamma$, the difference between the numerically calculated recovery point from the full model in the presence of abundance management and that predicted by the two-dimensional reduced model. The y-axis is the number of realizations of a random mutualistic network. Each network realization in (a) and (b) has 38 pollinators and 11 plants, and the approximate values of the connectance and nestedness are 0.25 and 0.36, respectively. Each network realization in (c) and (d) has 60 pollinators and 20 plants, and the value of the connectance is approximately 0.2. For (c) and (d), the values of nestedness are approximately 0.3 and 0.6, respectively. The control maintained abundance level is $A_S = 1.5$ for (a,c,d) and $A_S = 2$ for (b), and the managed species is the pollinator species with the largest mutualistic links to the plant species. The number of statistical realizations in all panels is 100. Other parameters have the same values as those in Fig. 1 in the main text.

reduced model is able to generate reasonably well prediction of the recovery point, but the prediction is poor for panels (c) and (d). A comparison of the results in panels (a) and (b) indicates that the value of the controlled abundance does not affect the predictive power of the reduced model.

Comparing the results in panels (a), (c), and (d), we find that the reduced model works surprisingly well for some mutualistic networks, but not so for some others. For example, the prediction is poorer for highly nested networks than for networks with a low degree of nestedness, as can be seen by comparing the results in panels (c) and (d). We can conclude that, in general, the reduced model tends to be more effective if the structure of the network is more random.

---

[1] J. Jiang, Z.-G. Huang, T. P. Seager, W. Lin, C. Grebogi, A. Hastings, and Y.-C. Lai, Proc. Natl. Acad. Sci. (USA) **115**, E639 (2018).

[2] E. H. van Nes and M. Scheffer, Amer. Nat. **164**, 255 (2004).

[3] J. J. Lever, E. H. Nes, M. Scheffer, and J. Bascompte, Ecol. Lett. **17**, 350 (2014).